Department of Mathematics and Statistics

12 September 2019

Boundary element methods for acoustic scattering by fractal screens

by

Simon N. Chandler-Wilde, David P. Hewett, Andrea Moiola and Jeanne Besson
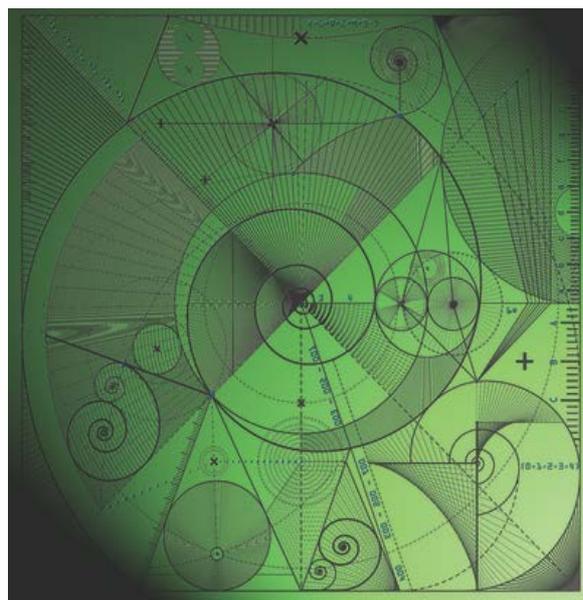
Boundary element methods for acoustic scattering by fractal screens

Simon N. Chandler-Wilde · David P.
Hewett · Andrea Moiola · Jeanne Besson

Abstract We study boundary element methods for time-harmonic scattering in $\mathbb{R}^n$ ($n = 2, 3$) by a fractal planar screen, assumed to be a non-empty bounded subset Γ of the hyperplane $\Gamma_\infty = \mathbb{R}^{n-1} \times \{0\}$. We consider two distinct cases: (i) Γ is a relatively open subset of Γ_∞ with fractal boundary (e.g. the interior of the Koch snowflake in the case $n = 3$); (ii) Γ is a compact fractal subset of Γ_∞ with empty interior (e.g. the Sierpinski triangle in the case $n = 3$). In both cases our numerical simulation strategy involves approximating the fractal screen Γ by a sequence of smoother "prefractal" screens, for which we compute the scattered field using boundary element methods that discretise the associated first kind boundary integral equations. We prove sufficient conditions on the mesh sizes guaranteeing convergence to the limiting fractal solution, using the framework of Mosco convergence. We also provide numerical examples illustrating our theoretical results.

Simon N. Chandler-Wilde
Department of Mathematics and Statistics, University of Reading, Whiteknights PO Box 220, Reading RG6 6AX, UK
E-mail: s.n.chandler-wilde@reading.ac.uk

David P. Hewett
Department of Mathematics, University College London, Gower Street, London, WC1E 6BT, UK
E-mail: d.hewett@ucl.ac.uk

Andrea Moiola
Dipartimento di Matematica, Università degli Studi di Pavia, Via Ferrata, 27100 Pavia, Italia
E-mail: andrea.moiola@unipv.it

Jeanne Besson
ENSTA Paris, 828 Boulevard des Maréchaux, 91120 Palaiseau, France
& Université Paris-Sud, 15 Rue Georges Clemenceau, 91400 Orsay, France
E-mail: jeanne.besson@ensta-paris.fr

1 Introduction

The scattering of acoustic waves by screens (or "cracks" in the elasticity literature) is a classical topic in physics, applied mathematics and scientific computing. The basic scattering problem involves an incident wave propagating in $\mathbb{R}^n$ ($n = 2$ or 3), striking a screen Γ, assumed to be a bounded subset (typically, a relatively open subset) of some $(n-1)$-dimensional submanifold of $\mathbb{R}^n$, and producing a scattered field which radiates outward to infinity. In a homogeneous background medium, the scattering problem can be reformulated as a boundary integral equation (BIE) on the screen, as described in e.g. [31, 38, 70, 71, 76], and numerical solutions can then be computed using the boundary element method (BEM), as in e.g. [42, 70, 71, 76]. The classical work cited above has since been extended in many directions, e.g. to the electromagnetic case [11, 14], to "multi-screens" (the union of multiple screens intersecting non-trivially) [28], and to hybrid numerical-asymptotic approximation spaces [40] for high-frequency problems.

For simplicity we focus on the case where the screen is flat, and the underlying $(n-1)$-dimensional submanifold is the hyperplane $\Gamma_\infty := \mathbb{R}^{n-1} \times \{0\} \subset \mathbb{R}^n$. Restricted to this setting, existing studies all assume (either explicitly or implicitly) that the screen $\Gamma \subset \Gamma_\infty$ is a (relatively) open set with smooth (or piecewise smooth) boundary. In our recent paper [24] we derived well-posed boundary value problem (BVP) and BIE formulations for sound-soft and sound-hard acoustic scattering by *arbitrary* bounded screens $\Gamma \subset \Gamma_\infty$, including cases where Γ or $\partial \Gamma$ has fractal structure. In this paper we consider the numerical solution of these BVPs/BIEs using the BEM.

Our focus is on scattering by two general classes of fractal screens[1]:

(i) Γ is a bounded, relatively open subset of Γ_∞ with fractal boundary, for instance the interior of the Koch snowflake in the case $n = 3$;

(ii) Γ is a compact fractal subset of Γ_∞ with empty relative interior, for instance the Sierpinski triangle in the case $n = 3$.

In both cases our general approach to analysis and numerical simulation is to approximate the fractal screen Γ by a sequence of smoother "prefractal" screens Γ_j, $j \in \mathbb{N}_0$, for which BVP/BIE well-posedness and BEM approximation is classical. The key question we address in this paper is:

Given a fractal screen Γ, how should the prefractals Γ_j and the corresponding BEM discretisations be chosen so as to ensure convergence of the numerical solutions on Γ_j to the limiting solution on Γ?

In this paper we focus exclusively on sound-soft screens, on which homogeneous Dirichlet boundary conditions are imposed. Our decision to restrict attention to this case was made partly to make numerical simulations as simple as possible, since one has only to discretise the weakly-singular single-layer boundary integral operator. But the sound-soft case is also particularly interesting from a physical point of view, as there is a strong dependence of the scattering properties on the fractal dimension of the screen (see Proposition 6.2 and the numerical results in §§7.3–7.4). We leave for future work the application of the techniques developed in

---

[1] While our focus in this paper is on fractal screens, our main results (for instance, Theorems 5.2 and 5.3) do not require fractality (neither self-similarity nor non-integer fractal dimension), but apply to any non-smooth screen approximated by a sequence of smoother screens.

this paper to the numerical simulation of the well-posed BVP/BIE formulations for scattering by fractal sound-hard and impedance screens presented in [23, 24, 39]. (See [23] for simulations of diffraction through fractal apertures in sound-hard screens, equivalent, by Babinet's Principle [12], to the sound-soft screen problem that we focus on in this paper.)

Our main results and their novelty. The main focus of this paper is to address the "key question" above, proving results (Theorems 5.2 and 5.3) that specify, for each of the classes (i) and (ii), how to choose a sequence of prefractals and their BEM discretisations so as to achieve convergence of the resulting numerical scheme to the limiting solution on Γ. While BEM simulations have been carried out previously on sequences of prefractals (see Jones et al. [48] in the context of potential theory and Panagiotopulos and Panagouli [59] in elasticity), prior to the results in this paper there does not appear to exist any analysis to justify the convergence of such simulations, that the sequence of numerical solutions converges to the desired limiting solution on Γ.

Our focus throughout the paper is on particular BIEs for sound-soft fractal screens, but we expect the methods and arguments that we introduce to be much more widely applicable. Indeed, our analysis is based on a variational formulation of the BIEs in terms of (complex-valued) continuous sesquilinear forms, which allows the question of prefractal to fractal convergence to be rephrased in terms of the Mosco convergence[2] of the discrete BEM subspaces to the fractional Sobolev space in which the limiting fractal solution lives. The methods that we develop, to reduce proof of convergence of the numerical solution to the Mosco convergence of the BEM subspaces (Lemma 2.5), and to prove Mosco convergence of the BEM subspaces, are potentially widely applicable to Galerkin discretisations of other integral or differential equations posed on rough (not necessarily fractal) domains that are approximated by more regular sets. For example, the proof of Theorem 5.3 depends only on a characterisation of Mosco convergence (Lemma 2.4), quantitative bounds on the norms of mollification operators on scales of Sobolev spaces (Appendix B), and a quantitative extension of standard piecewise constant finite element approximation theory (Lemma A.1), all of which should be widely applicable.

A feature of our numerical analysis based on Mosco convergence is that our discrete BEM subspaces need not be subspaces of the Hilbert space in which the solution on Γ lies; indeed, this is crucial whenever the prefractals are not subsets of the limiting fractal Γ. Our Lemma 2.5, which applies in such cases (and is proved in slightly more generality than we need for the results in §5, anticipating wider application) can be seen as a replacement in this circumstance for the standard Céa lemma and its generalisation to compact perturbations (see, e.g. [69, Thms. 8.10, 8.11]).

---

[2] Mosco convergence (Definition 2.2 below) is a standard notion in the study of variational inequalities, closely related to Gamma convergence. Introduced by U. Mosco in [54] (almost exactly 50 years ago), it has been applied by a number of authors to the study of PDEs on sequences of domains, see e.g. [13, 53] and the references therein. It has been mainly used (e.g. the references just cited) in relation to convergence at a continuous rather than a discrete level (i.e. in the context of mathematical analysis rather than numerical analysis). But it is also relevant to proving convergence of numerical methods, as was illustrated already in [55, Chapt. 3] in the context of numerical methods for variational inequalities.

While our main results, Theorems 5.2 and 5.3, are quite general in terms of geometry of the screen Γ and its approximating prefractal sequence, we pay particular attention in our theory, examples, and numerical simulations to cases where Γ (or the boundary of Γ) is the fixed point of an iterated function system (IFS) (e.g. Corollaries 4.6 and 5.8). In particular our examples in §6 and §7 include the cases where Γ is (when $n = 2$) a Cantor set and (when $n = 3$) a Cantor dust, the Sierpinski triangle, or the interior of a Koch snowflake. These are cases where the BIEs we wish to solve are posed either on fractal sets or on rough domains with fractal boundaries. Unsurprisingly, subtle and interesting properties of fractional Sobolev spaces and integral operators on rough sets, explored recently in [15, 22, 25, 26, 41], are crucial to our arguments throughout.

A novel feature of our BEM and its analysis is that convergence can be achieved in regimes where each boundary element contains many disjoint components of a prefractal (e.g. Corollary 5.8(ii) and Figure 1). To justify this we need an extension, that applies in such cases, of standard piecewise constant approximation theory in scales of Sobolev spaces with explicit constants. We supply this in Lemma A.1.

Applications and motivations. Wave scattering by fractal structures is relevant for numerous applications, since fractals provide a natural mathematical framework for modelling the multiscale roughness of many natural and man-made scatterers. We highlight in particular the propagation of acoustic and electromagnetic waves in dendritic structures like the human lung in medical science [1, 47], and the scattering of electromagnetic waves by snowflakes, ice crystals and other atmospheric particles in climate science [7, 20, 68, 74]. But particularly close to the fractal screen scattering problems that we focus on in this paper are configurations arising in the design of fractal antennas for electromagnetic wave transmission/reception (see e.g. [35, 61, 77]) and fractal piezoelectric ultrasound transducers (see e.g. [2, 3, 34, 57]) (fractal structures being attractive in these contexts because of the possibility of wideband performance), and configurations that arise in the study of fractal aperture problems in laser physics [27, 43, 46, 75]. The current study into acoustic scattering by fractal screens represents a first step towards the rigorous numerical analysis of integral equation methods for the study of such challenging problems involving fractal scatterers.

Related literature. One of the first studies of wave scattering by fractals appears to be M. Berry's 1979 paper [10] on scattering by "random phase screens", in which Berry coins the term "diffractal" to describe waves that have undergone interactions with fractal structures. The difficult problem of studying high frequency asymptotics for fractal scattering problems was investigated by Sleeman and Hua in [44, 65]. Concerning the study of PDE problems on fractal domains more generally, U. Mosco notes in [56] that *". . . introducing fractal constructions into the classic theory of PDEs opens a vast new field of study, both theoretically and numerically"*, but also that *"this new field has been only scratched"*. In addition to papers cited above, research that has started to explore this field of study includes work on finite element method approximations of heat transmission across fractal interfaces [5, 16, 18, 19, 51] and H^1 extension problems [32]; Dirichlet-to-Neumann (Poincaré-Steklov) operators on domains with fractal boundaries [4]; and finite difference [58] and conformal mapping [6] approaches to the computation of Laplace eigenfunctions on fractal domains.

Structure of the paper. In §2 we collect some important Hilbert and Sobolev space results that will be used throughout the paper. The main new result here is Lemma 2.5, which proves convergence of solutions of variational problems for "compactly perturbed coercive" sesquilinear forms on a Mosco-convergent sequence of closed subspaces. The compactly perturbed coercive setting is more general than we need for the particular problem under consideration in this paper, since for flat sound-soft screens the first-kind formulation is coercive (strongly elliptic) [22]. However, it is included here to lay the foundations for future investigations into other, closely related problems, such as curved sound-soft screens (as studied e.g. in [71, 76]), and impedance screens (as studied e.g. in [9, 39, 50]). In §3 we state well-posed BVPs and BIEs for open and closed screens, refining results from [24], and in §4 we prove convergence of solutions on prefractal screens to solutions on limiting fractal screens using the Mosco framework; in particular we prove for the first time convergence in cases where the prefractal sequence is not monotonic, and it holds neither that $\Gamma \subset \Gamma_j$ for all j, nor that $\Gamma_j \subset \Gamma$ for all j. In §5 we study numerical discretisations based on piecewise constant BEM approximations on prefractals, determining conditions under which the BEM solution converges to the limiting fractal solution in the joint limit of prefractal and mesh refinement. In §6 we present examples of the kind of fractal screens we have in mind, and in §7 we provide numerical results which illustrate our theoretical predictions through a number of concrete examples. We also include in this section preliminary numerical investigations into physical questions such as how the fractal dimension of a screen affects the magnitude of the resulting scattered field. In §8 we make a brief conclusion and list some of the many intriguing open problems.

2 Preliminaries

2.1 Dual space realisations

We say that a linear isomorphism between Hilbert spaces is *unitary* if it preserves the inner product (equivalently, if it is isometric [30, Prop. 5.2]). If H is a complex Hilbert space (as all the Hilbert spaces in this paper are) by its *dual space* H^* we mean, following Kato [49], the space of *anti-linear* continuous functionals on H. It is often convenient to identify H^*, itself a Hilbert space with the standard induced operator norm, with some other Hilbert space $\mathcal{H}$, termed a *realisation* of H^*. If $\langle \cdot, \cdot \rangle$ is a continuous sesquilinear form on $\mathcal{H} \times H$, and the mapping taking $\phi \in \mathcal{H}$ to $\ell_\phi \in H^*$, given by $\ell_\phi(\psi) = \langle \phi, \psi \rangle$, $\psi \in H$, is a unitary isomorphism, then we say that $\mathcal{H}$ is a *unitary realisation* of H^* with associated *duality pairing* $\langle \cdot, \cdot \rangle$. If $W \subset H$ is a closed subspace, then a unitary realisation of W^* is provided by the following simple but important result, e.g. [26, Lem. 2.2], which is a special case of a more general Banach space result, e.g. [63, Thm. 4.9].

Lemma 2.1. *Suppose that H and $\mathcal{H}$ are Hilbert spaces, and $\mathcal{H}$ is a unitary realisation of H^*, with duality pairing $\langle \cdot, \cdot \rangle$, and $W \subset H$ is a closed linear subspace. Set $\mathcal{W} := \left(W^{a, \mathcal{H}} \right)^{\perp} \subset \mathcal{H}$, where $\perp$ denotes orthogonal complement and*

$$W^{a, \mathcal{H}} := \{ \psi \in \mathcal{H} : \langle \psi, \phi \rangle = 0, \ \text{for all } \phi \in W \} \subset \mathcal{H}$$

is the annihilator of W in $\mathcal{H}$. *Then* $\mathcal{W}$ *is a unitary realisation of* W^*, *and its associated duality pairing is just the restriction to* $\mathcal{W} \times W$ *of the duality pairing on* $\mathcal{H} \times H$.

For a closed subspace $W \subset H$, $(W^\perp)^{a,\mathcal{H}} = (W^{a,\mathcal{H}})^\perp$ and $(W^{a,\mathcal{H}})^{a,H} = W$.

2.2 Variational problems

Suppose H is a Hilbert space with norm $\|\cdot\|_H$, and $a(\cdot,\cdot)$ is a sesquilinear form on $H \times H$ that is *continuous*, i.e., for some $C > 0$ (the *continuity constant*), $|a(u,v)| \leq C\|u\|_H\|v\|_H$, for all $u, v \in H$. To each such a, and each unitary realisation $\mathcal{H}$ of the dual space H^*, with associated duality pairing $\langle \cdot, \cdot \rangle$, there corresponds a unique bounded linear operator $A : H \to \mathcal{H}$ defined by

$$a(u,v) = \langle Au, v \rangle, \quad u, v \in H. \tag{1}$$

Conversely, every bounded linear operator $A : H \to \mathcal{H}$ defines via (1) an associated sesquilinear form $a(\cdot,\cdot)$ on $H \times H$.

We say that a and A are *coercive* if, for some $\alpha > 0$ (the *coercivity constant*),

$$|a(u,u)| \geq \alpha\|u\|_H^2, \quad \text{for all } u \in H.$$

We recall that A is compact, i.e. maps bounded sets to relatively compact sets, if and only if it is completely continuous, i.e., for every sequence $(u_j) \subset H$ and $u \in H$, $u_j \rightharpoonup u$ implies that $Au_j \to Au$. (Here $\to$ denotes norm convergence in $\mathcal{H}$ and $\rightharpoonup$ weak convergence in H.) We say that a is *compact* if A is compact: equivalently, if $a(u_j, v_j) \to a(u, v)$ whenever $(u_j) \subset H$, $(v_j) \subset H$ and $u, v \in H$ satisfy $u_j \rightharpoonup u$ and $v_j \rightharpoonup v$. We say that a and A are *compactly perturbed coercive* if $a = a_0 + a_1$ with a_0 coercive and a_1 compact; equivalently, $A = A_0 + A_1$ with A_0 coercive and A_1 compact. [3]

Let $W \subset H$ be a closed subspace of H and let $\mathcal{W} := (W^{a,\mathcal{H}})^\perp \subset \mathcal{H}$ be the unitary realisation of W^* provided by Lemma 2.1. We say that a is *invertible on* W if, for every $f \in \mathcal{W}$, the variational problem: find $u_W \in W$ such that

$$a(u_W, v) = \langle f, v \rangle, \quad \text{for all } v \in W, \tag{2}$$

has exactly one solution $u_W \in W$. This holds (e.g. [45, Thm. 2.15]) if and only if

$$\beta := \inf_{u \in W, \|u\|_H = 1} \sup_{v \in W, \|v\|=1} |a(u,v)| > 0 \quad \text{and} \quad \sup_{u \in W} |a(u,v)| > 0 \quad \forall v \in W \setminus \{0\}.$$

In terms of the associated operator A, (2) can be written equivalently as

$$P_{\mathcal{W}} A u = f, \tag{3}$$

where $P_{\mathcal{W}}$ is orthogonal projection in $\mathcal{H}$ onto $\mathcal{W}$, so that a is invertible on W if and only if $P_{\mathcal{W}} A|_W$ is invertible, in which case $\| (P_{\mathcal{W}} A|_W)^{-1} \| = \beta^{-1}$. If a is coercive then a is invertible on W by the Lax–Milgram lemma and $\beta \geq \alpha$. More generally, if a is compactly perturbed coercive, then a is invertible on W if and only if it is injective, meaning that the problem (2) has at most one solution $u_W \in W$ for every $f \in \mathcal{W}$.

---

[3] Terminology varies: what we call here *coercive* is often termed *H-elliptic* or *strongly elliptic*, and what we call here *compactly perturbed coercive* is often termed *coercive* (e.g. [69]).

2.3 Mosco convergence

We now consider the problem of approximating the solution of the variational problem (2) by the solutions of variational problems posed on a sequence of closed subspaces $(W_j)_{j=1}^\infty \subset H$. We say that a is *uniformly invertible* on such a sequence $(W_j)_{j=1}^\infty$ if a is invertible on W_j for all $j \in \mathbb{N}$ and the inverses are uniformly bounded, meaning that, for some constant $C > 0$ and all $j \in \mathbb{N}$ and $f_j \in \mathcal{W}_j := (W_j^{a,\mathcal{H}})^\perp$,

$$\|u_{W_j}\|_H \le C\|f_j\|_{\mathcal{W}_j},$$

where u_{W_j} is the unique solution of (2) with W replaced by W_j and f by f_j. Equivalently, a is uniformly invertible on (W_j) if $P_{\mathcal{W}_j} A|_{W_j}$ is invertible for $j \in \mathbb{N}$ and

$$\sup_{j \in \mathbb{N}} \left\| \left(P_{\mathcal{W}_j} A|_{W_j} \right)^{-1} \right\| < \infty.$$

Roughly speaking, given a variational problem (2), to ensure that the corresponding solutions on $(W_j)_{j=1}^\infty$ converge to the solution in W we require that a is sufficiently "well-behaved" and that W_j approximates W increasingly well as $j \to \infty$ in an appropriate sense. This statement is made precise in Lemma 2.5 for a compactly perturbed coercive and W_j converging to W in the Mosco sense. The following definition of Mosco convergence is precisely the notion of set convergence for convex sets introduced in [54, Definition 1.1], except that we specialise here from the general Banach space setting to the Hilbert space case, and our convex sets are specifically closed linear subspaces (as, for example, in [53]).

Definition 2.2 (Mosco convergence). *Let W and W_j, for $j \in \mathbb{N}$, be closed subspaces of a Hilbert space H. We say that W_j converges in the Mosco sense, or Mosco-converges, to W (written $W_j \xrightarrow{M} W$) if the following conditions hold:*

(i) For every $w \in W$ and $j \in \mathbb{N}$ there exists $w_j \in W_j$ such that $\|w_j - w\|_H \to 0$.
(ii) If (W_{j_m}) is a subsequence of (W_j), $w_m \in W_{j_m}$, for $m \in \mathbb{N}$, and $w_m \rightharpoonup w$ as $m \to \infty$, then $w \in W$.

Two simple cases in which Mosco convergence holds [54, Lems. 1.2 and 1.3] are

$$W_1 \subset W_2 \subset \cdots, \quad \text{with} \quad W = \overline{\bigcup_{j=1}^\infty W_j}, \quad \text{and} \tag{4}$$

$$W_1 \supset W_2 \supset \cdots \quad \text{with} \quad W = \bigcap_{j=1}^\infty W_j. \tag{5}$$

The following "sandwich lemma" is a trivial consequence of Definition 2.2.

Lemma 2.3. *If W_j^+, W_j^- and W_j are closed subspaces of H satisfying $W_j^- \subset W_j \subset W_j^+$ for each $j \in \mathbb{N}$, and both W_j^+ and W_j^- Mosco-converge to some closed subspace W of H, then W_j also Mosco-converges to W.*

The following lemma will also be useful. Again the proof is straightforward.

Lemma 2.4. *Let W_j and W be closed subspaces of H. To prove that $W_j \xrightarrow{M} W$ it suffices to show that (i) there exists a dense subspace $\widetilde{W} \subset W$ such that for every $w \in \widetilde{W}$ and $j \in \mathbb{N}$ there exists $w_j \in W_j$ such that $\|w_j - w\|_H \to 0$, and (ii) there*

exists a sequence of closed subspaces W_j^+ of H such that $W_j \subset W_j^+$ for all $j \in \mathbb{N}$ and $W_j^+ \xrightarrow{M} W$.

Mosco convergence was introduced to study convergence of approximate solutions to variational inequalities. The following lemma, which applies to variational *equalities*, appears to be new, but its proof, if specialised to the coercive case, has something of the flavour of the original arguments of Mosco [54, Thm. A and its Corollary]. Indeed, in the case that H is a real Hilbert space and a is coercive, this lemma is a corollary of the results in [54], since variational inequalities on linear subspaces of real Hilbert spaces are in fact equalities.

Lemma 2.5. *Let $W \subset H$ and $W_j \subset H$, for $j \in \mathbb{N}$, be closed subspaces such that W_j Mosco-converges to W as $j \to \infty$. Let a be compactly perturbed coercive and invertible on W. Then there exists $J \in \mathbb{N}$ such that a is uniformly invertible on W_j for $j \geq J$. Further, if, for some $f \in \mathcal{H}$, u_W denotes the solution to (2) and, for $j \geq J$, u_{W_j} denotes the solution to (2) with W replaced by W_j, then $\|u_{W_j} - u_W\|_H \to 0$ as $j \to \infty$.*

Proof. We show first that, for some $J \in \mathbb{N}$, a is uniformly invertible on W_j for $j \geq J$. Suppose first that a is not invertible on W_j for all sufficiently large j, in which case neither is it injective on W_j. Then there exists a subsequence of (W_j), which we will denote again by (W_j), and $v_j \in W_j$ with $\|v_j\|_H = 1$, such that

$$a(v_j, v) = 0, \quad v \in W_j. \tag{6}$$

If on the other hand a is invertible on W_j for all sufficiently large j but is not uniformly invertible then there exists a subsequence of (W_j), which we will denote again by (W_j), and $v_j \in W_j$ with $\|v_j\|_H = 1$ such that

$$\sup_{v \in W_j, \|v\|_H = 1} |a(v_j, v)| \to 0 \text{ as } j \to \infty. \tag{7}$$

In both of these cases as $\|v_j\|_H = 1$ is bounded we can extract a subsequence that is weakly convergent to some $v \in H$. Denoting the subsequence again by (v_j), we have that $v_j \in W_j$ and $v \in W$ by (ii) in Definition 2.2. Further, by (i) in Definition 2.2, for all $w \in W$, there exists a sequence $(w_j) \subset H$ with $w_j \in W_j$ such that $\|w_j - w\|_H \to 0$. Thus, and by (6) or (7),

$$a(v_j, w) = a(v_j, w_j) + a(v_j, w - w_j) \to 0 \text{ as } j \to \infty.$$

But also $a(v_j, w) \to a(v, w)$. Thus $a(v, w) = 0$ for all $w \in W$, so that $v = 0$ as a is invertible on W. So $v_j \rightharpoonup v = 0$ and, by (6) or (7), $a(v_j, v_j) \to 0$. Further, recalling that $a = a_0 + a_1$ with a_0 coercive and a_1 compact, we have also $a_1(v_j, v_j) \to 0$ as a_1 is compact. But this implies that $a_0(v_j, v_j) \to 0$, which contradicts that a_0 is coercive. Thus, for some $J \in \mathbb{N}$, a is invertible on W_j for $j \geq J$ and is uniformly bounded.

Thus, for $j \geq J$, u_{W_j} is well-defined and $(u_{W_j})_{j=J}^\infty$ is bounded and so has a weakly convergent subsequence, converging to a limit u_*, and $u_* \in W$ by (ii) in Definition 2.2. Further, by (i) in Definition 2.2, for all $w \in W$ there exists $w_j \in W_j$ such that $\|w_j - w\|_H \to 0$, and (2) gives

$$a(u_W, w) = \langle f, w \rangle = \langle f, w - w_j \rangle + \langle f, w_j \rangle = \langle f, w - w_j \rangle + a(u_{W_j}, w_j) \to a(u_*, w),$$

as $j \to \infty$ through that subsequence. Thus $a(u_W, w) = a(u_*, w)$, for all $w \in W$, so that $u_* = u_W$ by the invertibility of a on W. By the same argument every subsequence of $(u_{W_j})_{j=J}^{\infty}$ has a subsequence converging weakly to u_W, so that $(u_{W_j})_{j=J}^{\infty}$ converges weakly to u_W. Finally, we see that

$$a(u_{W_j} - u_W, u_{W_j} - u_W) = \langle f, u_{W_j} \rangle - a(u_{W_j}, u_W) - a(u_W, u_{W_j} - u_W) \to 0$$

as $j \to \infty$, by the weak convergence of $(u_{W_j})_{j=J}^{\infty}$ and (2). Since a_1 is compact, $a_1(u_{W_j} - u_W, u_{W_j} - u_W) \to 0$, so that also $a_0(u_{W_j} - u_W, u_{W_j} - u_W) \to 0$. Since a_0 is coercive it follows that $u_{W_j} \to u_W$. $\qquad\square$

Remark 2.6. *The statement of Lemma 2.5 can be strengthened if additional assumptions are made on a, $(W_j)_{j=1}^{\infty}$ and W.*

(i) *If a is coercive then one can take $J = 1$ (since a coercive sesquilinear form is automatically invertible on every subspace). In the special case when (5) holds, this was noted already in [26, Lem. 2.4].*
(ii) *If $W_j \subset W$ for each $j \in \mathbb{N}$ then (ii) in Definition 2.2 holds automatically and quasi-optimality holds asymptotically [69, Thms. 8.10-11], meaning that, for some $M > 0$ and $J \in \mathbb{N}$, a is invertible on W_j for $j \geq J$, and*

$$\|u_{W_j} - u_W\|_H \leq M \inf_{w_j \in W_j} \|u_W - w_j\|_H, \quad \text{for } j \geq J. \qquad (8)$$

Furthermore, if a is coercive then, by Céa's lemma, (8) holds with $J = 1$ and $M = C/\alpha$, where C and α are the continuity and coercivity constants for a.

2.4 Sobolev spaces and trace operators

Our notation follows that of [52] and [26]. Let $m \in \mathbb{N}$. For a subset $E \subset \mathbb{R}^m$ we denote its complement $E^c := \mathbb{R}^m \setminus E$, its closure $\overline{E}$ and its interior E°. We denote the Hausdorff (fractal) dimension of E by $\dim_H E$ (see, e.g., [72, §I.2]). We say that a non-empty closed set $F \subset \mathbb{R}^m$ is a d-set for some $0 \leq d \leq m$, if it is "uniformly d-dimensional", more precisely if there exist $c_1, c_2 > 0$ such that

$$c_1 r^d \leq \mathcal{H}^d\big(B_r(\mathbf{x}) \cap F\big) \leq c_2 r^d, \quad \mathbf{x} \in F, \ 0 < r \leq 1,$$

where $B_r(\mathbf{x})$ is the closed ball of radius r with centre at $\mathbf{x}$ and $\mathcal{H}^d$ denotes the d-dimensional Hausdorff measure on $\mathbb{R}^m$ [72, §I.3]. We say that a non-empty open set $\Omega \subset \mathbb{R}^m$ is C^0 (respectively Lipschitz) if its boundary $\partial\Omega$ can at each point be locally represented as the graph (suitably rotated) of a C^0 (respectively Lipschitz) function from $\mathbb{R}^{m-1}$ to $\mathbb{R}$, with Ω lying only on one side of $\partial\Omega$. For a more detailed definition see, e.g., [37, Defn 1.2.1.1]. For $m = 1$ these definitions coincide: we interpret them both to mean that Ω is a countable union of open intervals whose closures are disjoint and whose endpoints have no limit points.

For $s \in \mathbb{R}$, let $H^s(\mathbb{R}^m)$ denote the Hilbert space of tempered distributions whose Fourier transforms (defined for $\boldsymbol{\xi} \in \mathbb{R}^m$ as $\hat{u}(\boldsymbol{\xi}) := \frac{1}{(2\pi)^{m/2}} \int_{\mathbb{R}^m} e^{-i\boldsymbol{\xi}\cdot\mathbf{x}} u(\mathbf{x}) \, d\mathbf{x}$ in the case that $u \in C_0^{\infty}(\mathbb{R}^m)$) are locally integrable with

$$\|u\|_{H^s(\mathbb{R}^m)}^2 := \int_{\mathbb{R}^m} (1 + |\boldsymbol{\xi}|^2)^s |\hat{u}(\boldsymbol{\xi})|^2 \, d\boldsymbol{\xi} < \infty.$$

In particular, $H^0(\mathbb{R}^m) = L^2(\mathbb{R}^m)$ with equal norms. For the dual space of $H^s(\mathbb{R}^m)$ we have the unitary realisation $(H^s(\mathbb{R}^m))^* \cong H^{-s}(\mathbb{R}^m)$, with duality pairing

$$\langle u, v \rangle_{H^{-s}(\mathbb{R}^m) \times H^s(\mathbb{R}^m)} := \int_{\mathbb{R}^m} \hat{u}(\boldsymbol{\xi}) \overline{\hat{v}(\boldsymbol{\xi})} \, d\boldsymbol{\xi}, \tag{9}$$

which coincides with the $L^2(\mathbb{R}^m)$ inner product when both u and v are in $L^2(\mathbb{R}^m)$.

Given a closed set $F \subset \mathbb{R}^m$, we define

$$H_F^s := \{ u \in H^s(\mathbb{R}^m) : \operatorname{supp} u \subset F \},$$

and given a non-empty open set $\Omega \subset \mathbb{R}^m$, we define

$$\widetilde{H}^s(\Omega) := \overline{C_0^\infty(\Omega)}^{H^s(\mathbb{R}^m)},$$

the closure of $C_0^\infty(\Omega)$ in $H^s(\mathbb{R}^m)$. Clearly $\widetilde{H}^s(\Omega) \subset H_{\overline{\Omega}}^s$, and when Ω is sufficiently regular it holds that $\widetilde{H}^s(\Omega) = H_{\overline{\Omega}}^s$ (see Proposition 3.4 for results relevant to the current study); however, in general these spaces can be different [26, §3.5]. For non-empty open Ω we also define

$$H^s(\Omega) := \{ u = U|_\Omega \text{ for some } U \in H^s(\mathbb{R}^m) \},$$
$$\|u\|_{H^s(\Omega)} := \inf_{\substack{U \in H^s(\mathbb{R}^m) \\ U|_\Omega = u}} \|U\|_{H^s(\mathbb{R}^m)}.$$

Although $H^s(\Omega)$ is a space of distributions on Ω, it can be naturally identified with a space of distributions on $\mathbb{R}^m$, namely $(H_{\Omega^c}^s)^\perp \subset H^s(\mathbb{R}^m)$, where $^\perp$ denotes orthogonal complement in $H^s(\mathbb{R}^m)$, with the restriction operator $|_\Omega : (H_{\Omega^c}^s)^\perp \to H^s(\Omega)$ providing a unitary isomorphism between the two spaces.

Regarding duality, for arbitrary $F \subset \mathbb{R}^m$ closed and $\Omega \subset \mathbb{R}^m$ open, we can unitarily realise the dual spaces of H_F^s and $\widetilde{H}^s(\Omega)$ by certain closed subspaces of $H^{-s}(\mathbb{R}^m)$, with the duality pairing inherited from (9). Precisely, by Lemma 2.1,

$$(H_F^s)^* \cong (\widetilde{H}^{-s}(F^c))^\perp, \tag{10}$$

$$(\widetilde{H}^s(\Omega))^* \cong (H_{\Omega^c}^{-s})^\perp, \tag{11}$$

where $^\perp$ denotes orthogonal complement in $H^{-s}(\mathbb{R}^m)$, since [26, §3.2] $\widetilde{H}^{-s}(F^c)$ and $H_{\Omega^c}^{-s}$ are the annihilators of H_F^s and $\widetilde{H}^s(\Omega)$, respectively, with respect to the duality pairing (9). An alternative, and more widely-known unitary realisation of $(\widetilde{H}^s(\Omega))^*$ (also valid for arbitrary open $\Omega \subset \mathbb{R}^m$, see [26, Thm. 3.3]) is

$$(\widetilde{H}^s(\Omega))^* \cong H^{-s}(\Omega) \quad \text{with} \quad \langle u, v \rangle_{H^{-s}(\Omega) \times \widetilde{H}^s(\Omega)} := \langle U, v \rangle_{H^{-s}(\mathbb{R}^m) \times H^s(\mathbb{R}^m)}, \tag{12}$$

where $U \in H^{-s}(\mathbb{R}^m)$ is any extension of $u \in H^{-s}(\Omega)$ with $U|_\Omega = u$. That (11) and (12) are both unitary realisations of $(\widetilde{H}^s(\Omega))^*$ is consistent with the fact that $|_\Omega : (H_{\Omega^c}^{-s})^\perp \to H^{-s}(\Omega)$ is a unitary isomorphism, as mentioned above.

In the context of our screen scattering problem, we define Sobolev spaces on the hyperplane $\Gamma_\infty = \mathbb{R}^{n-1} \times \{0\}$ by associating Γ_∞ with $\mathbb{R}^{n-1}$ and setting $H^s(\Gamma_\infty) := H^s(\mathbb{R}^{n-1})$, for $s \in \mathbb{R}$, which we shall frequently abbreviate to simply H^s. For $E \subset \Gamma_\infty$ we set $\widetilde{E} := \{ \widetilde{\mathbf{x}} \in \mathbb{R}^{n-1} : (\widetilde{\mathbf{x}}, 0) \in E \} \subset \mathbb{R}^{n-1}$. Then for a closed

subset $F \subset \Gamma_\infty$ we define $H_F^s := H_{\widetilde{F}}^s \subset H^s$, and for a (relatively) open subset $\Omega \subset \Gamma_\infty$ we set $\widetilde{H}^s(\Omega) := \widetilde{H}^s(\widetilde{\Omega}) \subset H^s$ and $H^s(\Omega) := H^s(\widetilde{\Omega})$, etc. We stress that all Sobolev spaces on subsets of Γ_∞ such as H_F^s, $\widetilde{H}^s(\Omega)$ and $H^s(\Omega)$ are defined starting from $H^s = H^s(\Gamma_\infty) = H^s(\mathbb{R}^{n-1})$, as opposed to $H^s(\mathbb{R}^n)$; in other words, in the definitions earlier in this section we have $m = n - 1$.

In the exterior domain $D := \mathbb{R}^n \setminus \overline{\Gamma}$ we work with Sobolev spaces defined via weak derivatives. Given a non-empty open $\Omega \subset \mathbb{R}^n$, let $W^1(\Omega) := \{u \in L^2(\Omega) : \nabla u \in L^2(\Omega)\}$ and let $W^{1,\mathrm{loc}}(\Omega)$ denote the "local" space in which square integrability of u and ∇u is required only on bounded subsets of Ω. We note that, typically, $H^1(D) \subsetneq W^1(D)$, since the restriction space inherits from $H^1(\mathbb{R}^n)$ a requirement of (weak) continuity across Γ. We define $U^+ := \{(x_1, \dots, x_n) \in \mathbb{R}^n : x_n > 0\}$ and $U^- := \mathbb{R}^n \setminus \overline{U^+}$, and adopt the convention that the unit normal vector $\mathbf{n}$ on Γ_∞ points into U^+. From the half spaces $U^\pm$ to the hyperplane Γ_∞ we define the standard trace operators $\gamma^\pm : W^1(U^\pm) \to H^{1/2} = H^{1/2}(\Gamma_\infty)$ and $\partial_{\mathbf{n}}^\pm : \{u \in W^1(U^\pm) : \Delta u \in L^2(U^\pm)\} \to H^{-1/2} = H^{-1/2}(\Gamma_\infty)$. We shall frequently abuse notation and apply $\gamma^\pm$ and $\partial_{\mathbf{n}}^\pm$ to elements u of the local space $W^{1,\mathrm{loc}}(D)$, assuming implicitly that u has been pre-multiplied by a cutoff $\phi \in C_0^\infty(\mathbb{R}^n)$ satisfying $\phi = 1$ in some neighbourhood of $\overline{\Gamma}$, and restricted to $U^\pm$ as appropriate; for example, $\gamma^+ u$ should be interpreted as $\gamma^+((u\phi)|_{U^+})$.

3 Boundary value problems and boundary integral equations

Given a screen $\Gamma \subset \Gamma_\infty$ (a bounded subset of Γ_∞), and an incident wave $u^i \in H^{1,\mathrm{loc}}(\mathbb{R}^n)$ (for instance, a plane wave $u^i(\mathbf{x}) := \mathrm{e}^{\mathrm{i}k\mathbf{d}\cdot\mathbf{x}}$ with $\mathbf{d}$ a unit direction vector), we seek a scattered acoustic field u satisfying the Helmholtz equation

$$\Delta u + k^2 u = 0, \qquad k > 0, \tag{13}$$

in $D = \mathbb{R}^n \setminus \overline{\Gamma}$, the Sommerfeld radiation condition

$$\frac{\partial u(\mathbf{x})}{\partial r} - \mathrm{i}k u(\mathbf{x}) = o(r^{(1-n)/2}), \qquad r := |\mathbf{x}| \to \infty, \text{ uniformly in } \hat{\mathbf{x}} := \mathbf{x}/|\mathbf{x}|, \tag{14}$$

and the Dirichlet boundary condition

$$u = -u^i \qquad \text{on } \Gamma. \tag{15}$$

To formulate a well-posed BVP, one needs to be more precise about the sense in which the boundary condition (15) holds. A detailed investigation into this issue for general bounded subsets $\Gamma \subset \Gamma_\infty$ was carried out in [24]. Here we apply the results of [24] to describe well-posed BVP formulations for the two types of screen mentioned in the Introduction, namely (i) bounded, relatively open subsets of Γ_∞, and (ii) compact subsets of Γ_∞, possibly with empty relative interior. From now on, for brevity we shall omit the words "relative" and "relatively" when discussing relatively open subsets of Γ_∞ and relative complements, boundaries and interiors of subsets of Γ_∞.

3.1 Well-posed BVPs and BIEs for bounded open screens

Let Γ be a non-empty bounded open subset of Γ_∞. Then we can formulate the scattering BVP by imposing the Dirichlet boundary condition (15) by restriction to Γ (denoting this problem as $\mathsf{D}(\Gamma)^{\mathrm{r}}$, D for Dirichlet, r for restriction).

Definition 3.1 (Problem $\mathsf{D}(\Gamma)^{\mathrm{r}}$ for bounded open screens). *Let $\Gamma \subset \Gamma_\infty$ be non-empty, bounded and open. Given $g^{\mathrm{r}} \in H^{1/2}(\Gamma)$ (specifically $g^{\mathrm{r}} := -(\gamma^\pm u^i)|_\Gamma$ for the scattering problem), find $u \in C^2(D) \cap W^{1,\mathrm{loc}}(D)$ satisfying (13) in D, (14), and*

$$(\gamma^\pm u)|_\Gamma = g^{\mathrm{r}}.$$

A well-posedness result for this formulation is provided in Theorem 3.2, which is proved in [24, Thm. 6.2(a)]. Before stating it we need some more notation. For $\Gamma \subset \Gamma_\infty$ non-empty, bounded and open let $\mathcal{S}_\Gamma : \widetilde{H}^{-1/2}(\Gamma) \to C^2(D) \cap W^{1,\mathrm{loc}}(\mathbb{R}^n)$ denote the standard single-layer potential, defined for $\phi \in C_0^\infty(\Gamma)$ by

$$\mathcal{S}_\Gamma \phi(\mathbf{x}) = \int_\Gamma \Phi(\mathbf{x}, \mathbf{y}) \phi(\mathbf{y}) \, \mathrm{d}s(\mathbf{y}), \qquad \mathbf{x} \in D, \tag{16}$$

with $\Phi(\mathbf{x}, \mathbf{y}) = \mathrm{e}^{\mathrm{i}k|\mathbf{x}-\mathbf{y}|}/(4\pi|\mathbf{x}-\mathbf{y}|)$ $(n = 3)$ or $\Phi(\mathbf{x}, \mathbf{y}) = (\mathrm{i}/4)H_0^{(1)}(k|\mathbf{x}-\mathbf{y}|)$ $(n = 2)$, and $S_\Gamma^{\mathrm{r}} : \widetilde{H}^{-1/2}(\Gamma) \to H^{1/2}(\Gamma)$ the single layer boundary integral operator (BIO), the bounded linear operator defined by

$$S_\Gamma^{\mathrm{r}} \phi := (\gamma^\pm \mathcal{S}_\Gamma \phi)|_\Gamma. \tag{17}$$

Theorem 3.2 ([24, Thm. 6.2(a)], [15, Lem. 4.15(ii)]). *Let $\Gamma \subset \Gamma_\infty$ be non-empty, bounded and open, with $\widetilde{H}^{-1/2}(\Gamma) = H_{\overline{\Gamma}}^{-1/2}$. Then problem $\mathsf{D}(\Gamma)^{\mathrm{r}}$ has a unique solution. Moreover, it satisfies the representation formula*

$$u(\mathbf{x}) = -\mathcal{S}_\Gamma \phi(\mathbf{x}), \qquad \mathbf{x} \in D, \tag{18}$$

where $\phi = \partial_{\mathbf{n}}^+ u - \partial_{\mathbf{n}}^- u \in \widetilde{H}^{-1/2}(\Gamma)$ is the unique solution of the BIE

$$S_\Gamma^{\mathrm{r}} \phi = -g^{\mathrm{r}}. \tag{19}$$

Remark 3.3. *The statement of [24, Thm. 6.2(a)] includes an extra assumption that $H_{\partial\Gamma}^{1/2} = \{0\}$, where $\partial\Gamma$ denotes the relative boundary of $\Gamma \subset \Gamma_\infty$. But this extra assumption is superfluous, since by [15, Lem. 4.15(ii)] it follows automatically from the assumption that $\widetilde{H}^{-1/2}(\Gamma) = H_{\overline{\Gamma}}^{-1/2}$.*

The key condition for the well-posedness in Theorem 3.2 is $\widetilde{H}^{-1/2}(\Gamma) = H_{\overline{\Gamma}}^{-1/2}$; the next proposition gives sufficient conditions on Γ for this to hold.

Proposition 3.4. *Each of the following are sufficient for $\widetilde{H}^{-1/2}(\Gamma) = H_{\overline{\Gamma}}^{-1/2}$:*

(i) Γ is C^0 (which holds in particular if Γ is Lipschitz) [52, Thm. 3.29];
(ii) Γ is C^0 except at a set of countably many points $P \subset \partial\Gamma$ such that P has only finitely many limit points [26, Thm. 3.24];
(iii) $|\partial\Gamma| = 0$, where $|\cdot|$ denotes Lebesgue measure on $\Gamma_\infty \cong \mathbb{R}^{n-1}$, and Γ is "thick" in the sense of Triebel ([15, Def. 4.5(iii)] or [73, Def. 3.1(ii)(iv), Rem. 3.2]).

In §6 we shall combine Theorem 3.2 and Proposition 3.4 to obtain well-posed-ness results for three-dimensional scattering by certain generalisations of the classical Koch snowflake, as immediate corollaries of the recently established thickness results in [15] (which build on earlier results in [73, Prop. 3.8(iii)]). We shall also deduce well-posedness results for scattering by the standard prefractal approximations to various well-known fractals including the Koch snowflake (and its generalisations), the Sierpinski triangle, and the Cantor dust. In all these cases the standard prefractals are either C^0 or C^0 except at a finite set of points.

Recalling from §2.4 that $|_\Gamma : (H^{1/2}_{\Gamma^c})^\perp \to H^{1/2}(\Gamma)$ is a unitary isomorphism, we note that the problem $\mathsf{D}(\Gamma)^\mathsf{r}$ can be equivalently stated with the boundary condition (15) imposed by orthogonal projection. (See Remark 3.6 below for an explanation of why this makes sense physically.) It is instructive to write down this equivalent formulation explicitly, since we will adopt a similar viewpoint when defining BVPs for scattering by compact screens in §3.2. In the following let $P_\Gamma : H^{1/2} \to (H^{1/2}_{\Gamma^c})^\perp$ denote orthogonal projection and define $S_\Gamma : \widetilde{H}^{-1/2}(\Gamma) \to (H^{1/2}_{\Gamma^c})^\perp$ by $S_\Gamma := P_\Gamma \gamma^\pm \mathcal{S}_\Gamma$.

Definition 3.5 (Problem $\mathsf{D}(\Gamma)$ for bounded open screens). *Let $\Gamma \subset \Gamma_\infty$ be non-empty, bounded and open. Given $g \in (H^{1/2}_{\Gamma^c})^\perp$ (specifically $g := -P_\Gamma \gamma^\pm u^i$ for the scattering problem), find $u \in C^2(D) \cap W^{1,\mathrm{loc}}(D)$ satisfying (13) in D, (14), and the boundary condition*

$$P_\Gamma \gamma^\pm u = g. \tag{20}$$

Remark 3.6. *To understand why the boundary condition (20) makes sense in the scattering problem, let $u^t := u + u^i$ be the total field (the sum of the scattered and incident fields), and consider the traces $\gamma^\pm u^t$ of u^t on $\Gamma_\infty \supset \Gamma$. According to formulation $\mathsf{D}(\Gamma)^\mathsf{r}$ these traces vanish on Γ, so their support lies in the complement Γ^c, i.e. $\gamma^\pm u^t \in H^{1/2}_{\Gamma^c}$ (more precisely $\gamma^\pm(\chi u^t) \in H^{1/2}_{\Gamma^c}$ for every $\chi \in C_0^\infty(\mathbb{R}^n)$ with $\chi = 1$ in a neighbourhood of $\overline{\Gamma}$). But since the kernel of P_Γ is $H^{1/2}_{\Gamma^c}$, this is equivalent to $P_\Gamma \gamma^\pm u^t = 0$ (more precisely $P_\Gamma \gamma^\pm(\chi u^t) = 0$), which is just (20) with $g := -P_\Gamma \gamma^\pm u^i$.*

Since the restriction operator $|_\Gamma : (H^{-1/2}_{\Gamma^c})^\perp \to H^{-1/2}(\Gamma)$ is unitary, the following proposition is a restatement of Theorem 3.2.

Proposition 3.7. *Problems $\mathsf{D}(\Gamma)^\mathsf{r}$ and $\mathsf{D}(\Gamma)$ are equivalent, under the identification $g^\mathsf{r} = g|_\Gamma$. Furthermore, when $\widetilde{H}^{-1/2}(\Gamma) = H^{-1/2}_{\overline{\Gamma}}$ the common unique solution of both problems can be represented as (18) where $\phi = \partial_\mathbf{n}^+ u - \partial_\mathbf{n}^- u \in \widetilde{H}^{-1/2}(\Gamma)$ is the common unique solution of the BIE (19) and the BIE*

$$S_\Gamma \phi = -g. \tag{21}$$

3.2 Well-posed BVPs and BIEs for compact screens

Now let $\Gamma \subset \Gamma_\infty$ be compact. In particular we have in mind the case where Γ has empty interior, in which case it is not possible to impose the boundary condition (15) by restriction. But, inspired by Definition 3.5 and Proposition 3.7, we can impose (15) by an appropriate orthogonal projection; we justify this in

Remark 3.9 below. Extending our existing notation, for compact Γ let P_Γ denote the orthogonal projection $P_\Gamma : H^{1/2} \to (\widetilde{H}^{1/2}(\Gamma^c))^\perp$.

Definition 3.8 (Problem $\mathsf{D}(\Gamma)$ for compact screens)**.** *Let $\Gamma \subset \Gamma_\infty$ be non-empty and compact. Given $g \in (\widetilde{H}^{1/2}(\Gamma^c))^\perp$ (specifically $g := -P_\Gamma \gamma^\pm u^i$ for the scattering problem), find $u \in C^2(D) \cap W^{1,\mathrm{loc}}(D)$ satisfying (13) in D, (14), and*

$$P_\Gamma \gamma^\pm u = g. \tag{22}$$

Remark 3.9. *We can justify the formulation in Definition 3.8, in particular (22), by relating it to a more familiar formulation of the scattering problem for compact screens [24, Defn. 3.1] that replaces (22) with the requirement that $u^t := u + u^i \in W_0^{1,\mathrm{loc}}(D)$, where $W_0^{1,\mathrm{loc}}(D)$ is the "local" version of $W_0^1(D)$, and $W_0^1(D)$ is the closure of $C_0^\infty(D)$ in $W^1(D)$. This formulation is well-posed [24, Thm 3.1] when Γ is any compact subset of $\mathbb{R}^n$. In the particular case when $\Gamma \subset \Gamma_\infty$ is a screen it is easy to see that $u^t \in W_0^{1,\mathrm{loc}}(D)$ implies that $\gamma^\pm u^t \in \widetilde{H}^{1/2}(\Gamma^c)$ (more accurately $\gamma^\pm(\chi u^t) \in \widetilde{H}^{1/2}(\Gamma^c)$ for every $\chi \in C_0^\infty(\mathbb{R}^n)$ with $\chi = 1$ in a neighbourhood of Γ). But since the kernel of P_Γ is $\widetilde{H}^{1/2}(\Gamma^c)$, this is equivalent to $P_\Gamma \gamma^\pm u^t = 0$ (more precisely $P_\Gamma \gamma^\pm(\chi u^t) = 0$), which is just (22) with $g := -P_\Gamma \gamma^\pm u^i$.*

Before stating a well-posedness result for this formulation (which we do in Theorem 3.10), we need some more notation. Given $\Gamma \subset \Gamma_\infty$ compact and $\epsilon > 0$, let $\Gamma(\epsilon) := \{\mathbf{x} \in \Gamma_\infty : \mathrm{dist}(\mathbf{x}, \Gamma) < \epsilon\}$ and $D_\epsilon := \mathbb{R}^n \setminus \overline{\Gamma(\epsilon)}$. Define $\mathcal{S}_{\Gamma(\epsilon)} : \widetilde{H}^{-1/2}(\Gamma(\epsilon)) \to C^2(D_\epsilon) \cap W^{1,\mathrm{loc}}(\mathbb{R}^n)$ by (16) with Γ replaced by $\Gamma(\epsilon)$. Define $\mathcal{S}_\Gamma : H_\Gamma^{-1/2} \to C^2(D) \cap W^{1,\mathrm{loc}}(\mathbb{R}^n)$ by $\mathcal{S}_\Gamma \phi(\mathbf{x}) := \mathcal{S}_{\Gamma(\epsilon)} \phi(\mathbf{x})$ for $\mathbf{x} \in D$ and $0 < \epsilon < \mathrm{dist}(\mathbf{x}, \Gamma)$, which is well-defined and independent of $\epsilon > 0$ since $H_\Gamma^{-1/2} \subset \widetilde{H}^{-1/2}(\Gamma(\epsilon))$ for every $\epsilon > 0$. Define $S_\Gamma : H_\Gamma^{-1/2} \to (\widetilde{H}^{1/2}(\Gamma^c))^\perp$ by $S_\Gamma := P_\Gamma \gamma^\pm \mathcal{S}_\Gamma$.

Theorem 3.10 ([24, Thm. 3.29 and Thm. 6.4])**.** *Let $\Gamma \subset \Gamma_\infty$ be non-empty and compact. Then problem $\mathsf{D}(\Gamma)$ has a unique solution satisfying the representation formula (18), where $\phi = \partial_{\mathbf{n}}^+ u - \partial_{\mathbf{n}}^- u \in H_\Gamma^{-1/2}$ is the unique solution of the BIE*

$$S_\Gamma \phi = -g.$$

Remark 3.11. *Suppose that $\Gamma \subset \Gamma_\infty$ is non-empty, bounded and open, in which case $\overline{\Gamma}$ is compact, and suppose also that $\widetilde{H}^{-1/2}(\Gamma) = H_{\overline{\Gamma}}^{-1/2}$. Then we have a choice of well-posed formulations for the scattering problem, potentially with different solutions: problem $\mathsf{D}(\Gamma)$ (see Definition 3.5) with $g := -P_\Gamma \gamma^\pm u^i$ (equivalently, $\mathsf{D}(\Gamma)^r$ with $g^r := -(\gamma^\pm u^i)|_\Gamma$) and problem $\mathsf{D}(\overline{\Gamma})$ (see Definition 3.8) with $g := -P_{\overline{\Gamma}} \gamma^\pm u^i$. But the assumption that $\widetilde{H}^{-1/2}(\Gamma) = H_{\overline{\Gamma}}^{-1/2}$ implies (in fact, is equivalent to) $\widetilde{H}^{1/2}(\overline{\Gamma}^c) = H_{\Gamma^c}^{1/2}$ (see [26, Lem. 3.26] and the proof of [15, Lem. 4.15]), and from this it follows that $\mathcal{S}_{\overline{\Gamma}} = \mathcal{S}_\Gamma$, $P_{\overline{\Gamma}} = P_\Gamma$, and $S_{\overline{\Gamma}} = S_\Gamma = |_\Gamma^{-1} \circ S_\Gamma^r$. So the two problems $\mathsf{D}(\Gamma)$ and $\mathsf{D}(\overline{\Gamma})$ are equivalent, sharing the same unique solution.*

It is natural to ask whether, in the case where $\Gamma \subset \Gamma_\infty$ is compact with empty interior, the screen scatters waves at all. This question was answered in [24].

Proposition 3.12 ([24, Thm. 4.6])**.**   *Let $\Gamma \subset \Gamma_\infty$ be non-empty and compact. If $H_\Gamma^{-1/2} = \{0\}$ then the solution of $\mathsf{D}(\Gamma)$ satisfies $u = 0$ for all $g \in (\widetilde{H}^{1/2}(\Gamma^c))^\perp$*

(and so for all incident waves u^i). If $H_\Gamma^{-1/2} \neq \{0\}$ and $0 \neq g \in (\widetilde{H}^{1/2}(\Gamma^c))^\perp$ (in particular, if $g = -P_\Gamma \gamma^\pm u^i$ and u^i is C^∞ in a neighbourhood of Γ with $u^i(\mathbf{x}) \neq 0$ for all $\mathbf{x} \in \Gamma$) then $u \neq 0$.

The question of whether $H_K^s = \{0\}$ for given $s \in \mathbb{R}$ and compact $K \subset \mathbb{R}^m$ was investigated in detail in [41]. For sets of Lebesgue measure zero, the Hausdorff dimension $\dim_H K$ provides partial characterisation. Specifically, if $s > (\dim_H K - m)/2$ then $H_K^s = \{0\}$, and if $s < (\dim_H K - m)/2$ then $H_K^s \neq \{0\}$. For $s = (\dim_H K - m)/2$ both behaviours are possible. But if K is a d-set for some $0 \leq d < m$ (see §2.4 for definition) then $H_K^{(d-m)/2} = \{0\}$. For such d-sets, the question of whether H_K^t is dense in H_K^s for $s < t < (d-m)/2$ was investigated in [15]. The following lemma collects the results from [15,41] relevant to our current purposes, translated to our spaces H_Γ^s, where $\Gamma \subset \Gamma_\infty = \mathbb{R}^{n-1} \times \{0\}$.

Lemma 3.13 ([41, Thms. 2.12, 2.17, Cor. 2.16], [15, Prop. 3.7(i), Thm. 6.14]). *Let $\Gamma \subset \Gamma_\infty = \mathbb{R}^{n-1} \times \{0\}$ ($n = 2, 3$) be compact. If $d := \dim_H(\Gamma) > n - 2$ then $H_\Gamma^t \neq \{0\}$ for $-1/2 \leq t < (d - n + 1)/2$. If Γ is countable, or if $n = 3$ and $\dim_H(\Gamma) < n - 2$ or Γ is an $(n-2)$-set, then $H_\Gamma^{-1/2} = \{0\}$. Furthermore, if Γ is a compact d-set for some $n - 2 < d < n - 1$ then $H_\Gamma^t \neq \{0\}$ is dense in $H_\Gamma^{-1/2} \neq \{0\}$ for $-1/2 \leq t < (d - n + 1)/2$.*

3.3 Variational formulations of the BIEs

To state and analyse Galerkin methods for the BIE formulations, in particular to use the Mosco convergence theory of §2.3, we need variational formulations.

When Γ is a bounded open set and $\widetilde{H}^{-1/2}(\Gamma) = H_{\overline{\Gamma}}^{-1/2}$, or when Γ is compact, we have written down, in Proposition 3.7 and Theorem 3.10, BIEs that are equivalent to the corresponding BVP formulation $\mathsf{D}(\Gamma)$. In each case these take the form (21), i.e. $S_\Gamma \phi = -g$. In this equation $\phi \in V(\Gamma)$, where

$$V(\Gamma) = \begin{cases} \widetilde{H}^{-1/2}(\Gamma) & \text{if } \Gamma \text{ is bounded and open,} \\ H_\Gamma^{-1/2} & \text{if } \Gamma \text{ is compact,} \end{cases} \tag{23}$$

and $g \in V(\Gamma)^*$, where $V(\Gamma)^*$ is a unitary realisation of the dual space of $V(\Gamma)$, specifically $V(\Gamma)^* = (H_{\Gamma^c}^{1/2})^\perp$ or $V(\Gamma)^* = (\widetilde{H}^{1/2}(\Gamma^c))^\perp$, in the respective cases. In each case $S_\Gamma : V(\Gamma) \to V(\Gamma)^*$ is a bounded linear operator, a version of the single-layer potential operator.

As noted in §2.2, S_Γ has an associated sesquilinear form $a_\Gamma(\cdot, \cdot)$ defined by

$$a_\Gamma(\phi, \psi) := \langle S_\Gamma \phi, \psi \rangle_{V(\Gamma)^* \times V(\Gamma)}, \quad \phi, \psi \in V(\Gamma).$$

Further (see §2.4), the duality pairing on $V(\Gamma)^* \times V(\Gamma)$ is simply the restriction to $V(\Gamma)^* \times V(\Gamma)$ of the duality pairing (9) on $H^{1/2} \times H^{-1/2}$. Thus, for $\phi, \psi \in V(\Gamma)$,

$$a_\Gamma(\phi, \psi) = \langle S_\Gamma \phi, \psi \rangle_{H^{1/2} \times H^{-1/2}} = \langle \gamma^\pm \mathcal{S}_\Gamma \phi, \psi \rangle_{H^{1/2} \times H^{-1/2}}. \tag{24}$$

The second equality in (24) holds since $S_\Gamma = P_\Gamma \gamma^\pm \mathcal{S}_\Gamma$, where P_Γ is orthogonal projection onto $V(\Gamma)^*$, and since $(V(\Gamma)^*)^\perp$ is the annihilator of $V(\Gamma)$, as noted below (11).

A consequence of (24) and the definition of $\mathcal{S}_\Gamma$ is that, if $\Gamma_\dagger \subset \Gamma_\infty$ is any bounded open set containing Γ, in which case $V(\Gamma)$ is a closed subspace of $\widetilde{H}^{-1/2}(\Gamma_\dagger)$, then

$$a_\Gamma(\phi,\psi) = \langle \gamma^\pm \mathcal{S}_{\Gamma_\dagger}\phi, \psi \rangle_{H^{1/2} \times H^{-1/2}} = a_{\Gamma_\dagger}(\phi,\psi), \quad \phi, \psi \in V(\Gamma), \qquad (25)$$

i.e. $a_\Gamma(\cdot,\cdot)$ is the restriction to $V(\Gamma)$ of $a_{\Gamma_\dagger}(\cdot,\cdot)$. Since we can choose $\Gamma_\dagger$ to be as smooth as we wish, e.g. C^∞, or indeed just an open disk, we see that, even when Γ is fractal or has fractal boundary, the sesquilinear forms we have to deal with are no more complicated than in the case when Γ is a disk.

A further consequence of (24) is that, in the case when Γ is bounded and open,

$$a_\Gamma(\phi,\psi) = \langle (\gamma^\pm \mathcal{S}_\Gamma\phi)|_\Gamma, \psi \rangle_{H^{1/2}(\Gamma) \times \widetilde{H}^{-1/2}(\Gamma)}, \quad \phi, \psi \in V(\Gamma) = \widetilde{H}^{-1/2}(\Gamma), \quad (26)$$

so that, where S_Γ^{r} is the more familiar screen single-layer potential operator defined by (17), $a_\Gamma(\cdot,\cdot)$ is also the sesquilinear form associated to S_Γ^{r}.

Whether Γ is bounded and open or is compact, the sesquilinear form $a_\Gamma(\cdot,\cdot)$ is continuous. Further, as a consequence of our assumption that the screen is flat (i.e. $\Gamma \subset \Gamma_\infty = \mathbb{R}^{n-1} \times \{0\}$), it is coercive. For the bounded open case this is hinted at in [38, Rem. 6] and proved rigorously in [22], the latter reference also detailing the wavenumber-dependence of the continuity and coercivity constants. That coercivity of $a_\Gamma(\cdot,\cdot)$ holds also for every compact Γ is a simple consequence of (25), since coercivity implies coercivity on every closed subspace.

As noted in the general Hilbert space setting in §2.2 (see (2) and (3)), the variational problem: given $g \in V(\Gamma)^*$

$$\text{find } \phi \in V(\Gamma) \text{ s.t. } a_\Gamma(\phi,\psi) = -\langle g, \psi \rangle_{V(\Gamma)^* \times V(\Gamma)}, \quad \forall \psi \in V(\Gamma), \qquad (27)$$

is equivalent to the BIE $S_\Gamma\phi = -g$. The duality pairing on the right hand side can be written equivalently as

$$\langle g, \psi \rangle_{V(\Gamma)^* \times V(\Gamma)} = \langle g, \psi \rangle_{H^{1/2} \times H^{-1/2}}.$$

Since $a_\Gamma(\cdot,\cdot)$ is coercive, (27) is well-posed by the Lax–Milgram lemma.

4 Prefractal to fractal convergence

Now suppose we want to study a sequence of problems on a sequence of screens $(\Gamma_j)_{j \in \mathbb{N}_0}$ (each non-empty and either bounded and open or compact) approximating a limiting screen Γ (again, non-empty and either bounded and open or compact). Assuming that the Γ_j are uniformly bounded, let $\Gamma_\dagger \subset \Gamma_\infty$ be a bounded open set (e.g. a disk) such that $\Gamma \subset \Gamma_\dagger$ and $\Gamma_j \subset \Gamma_\dagger$ for each $j \in \mathbb{N}_0$. Let $g_\dagger \in (H_{\Gamma_\dagger^c}^{1/2})^\perp \subset H^{1/2}$ be fixed. Then by the continuity and coercivity of the sesquilinear form $a_{\Gamma_\dagger}(\cdot,\cdot)$ (discussed in §3.3), for any closed subspaces V_j and V of $V(\Gamma_\dagger) = \widetilde{H}^{-1/2}(\Gamma_\dagger)$ the variational problems

$$\text{find } \phi \in V \text{ s.t. } a_{\Gamma_\dagger}(\phi,\psi) = -\langle g_\dagger, \psi \rangle_{H^{1/2} \times H^{-1/2}}, \quad \forall \psi \in V, \qquad (28)$$

$$\text{find } \phi_j \in V_j \text{ s.t. } a_{\Gamma_\dagger}(\phi_j,\psi) = -\langle g_\dagger, \psi \rangle_{H^{1/2} \times H^{-1/2}}, \quad \forall \psi \in V_j, \qquad (29)$$

are well-posed. The following theorem follows from Lemma 2.5, combined with the continuity of $\mathcal{S}_{\Gamma_\dagger} : \widetilde{H}^{-1/2}(\Gamma_\dagger) \to W^{1,\mathrm{loc}}(\mathbb{R}^n)$ (defined by (16)).

Theorem 4.1. *Let V_j and V be closed subspaces of $V(\Gamma_\dagger) = \widetilde{H}^{-1/2}(\Gamma_\dagger)$ and let $\phi \in V$ and $\phi_j \in V_j$ denote the solutions of (28) and (29) respectively. If $V_j \xrightarrow{M} V$ as $j \to \infty$ then $\phi_j \to \phi$ as $j \to \infty$ in $\widetilde{H}^{-1/2}(\Gamma_\dagger)$, and hence $\mathcal{S}_{\Gamma_j}\phi_j = \mathcal{S}_{\Gamma_\dagger}\phi_j \to \mathcal{S}_{\Gamma_\dagger}\phi = \mathcal{S}_\Gamma\phi$ as $j \to \infty$ in $W^{1,\mathrm{loc}}(\mathbb{R}^n)$.*

Definition 4.2 (BVP convergence). *Suppose that Γ is non-empty and either bounded and open or compact, and that the sequence $(\Gamma_j)_{j \in \mathbb{N}_0}$ is uniformly bounded, and that each Γ_j is non-empty and either bounded and open or compact. Then we say that "BVP convergence holds" if $V_j \xrightarrow{M} V$ as $j \to \infty$, where $V := V(\Gamma)$ and $V_j := V(\Gamma_j)$, with $V(\cdot)$ defined as in (23).*

The rationale behind this terminology is that, with these conditions on Γ and Γ_j, if $V_j \xrightarrow{M} V$, then it follows by Theorem 4.1 that $\phi_j \to \phi$ in $H^{-1/2}$, where ϕ and ϕ_j are the solutions to (28) and (29), respectively, and that $\mathcal{S}_{\Gamma_j}\phi_j \to \mathcal{S}_\Gamma\phi$ in $W^{1,\mathrm{loc}}(\mathbb{R}^n)$, where (noting (25) and the equivalence of (26) with the BIE) $\mathcal{S}_\Gamma\phi$ and $\mathcal{S}_{\Gamma_j}\phi_j$ are the unique solutions to the BVPs $\mathsf{D}(\Gamma)$ and $\mathsf{D}(\Gamma_j)$, with data $g := P_\Gamma g_\dagger$ and $g_j := P_{\Gamma_j}g_\dagger$. In particular, $\mathcal{S}_\Gamma\phi$ and $\mathcal{S}_{\Gamma_j}\phi_j$ are the scattered fields for scattering of the incident field u^i by Γ and Γ_j, respectively, provided $g_\dagger := -P_{\Gamma_\dagger}\gamma^\pm u^i$.

Sufficient conditions guaranteeing BVP convergence are given in the following proposition, which follows trivially from (4), (5), [26, Props. 3.33 and 3.34] and the "sandwich lemma" of Mosco convergence, Lemma 2.3.

Proposition 4.3. *$V_j \xrightarrow{M} V$ in any of the three following situations:*

(i) **(increasing open)** *$V := V(\Gamma) = \widetilde{H}^{-1/2}(\Gamma)$ and $V_j := V(\Gamma_j) = \widetilde{H}^{-1/2}(\Gamma_j)$, where Γ and Γ_j are non-empty, bounded and open with $\Gamma_j \subset \Gamma_{j+1}$, $j \in \mathbb{N}_0$, and $\Gamma = \bigcup_{j \in \mathbb{N}_0} \Gamma_j$;*

(ii) **(decreasing compact)** *$V := V(\Gamma) = H_\Gamma^{-1/2}$ and $V_j := V(\Gamma_j) = H_{\Gamma_j}^{-1/2}$, where Γ and Γ_j are non-empty and compact with $\Gamma_j \supset \Gamma_{j+1}$, $j \in \mathbb{N}_0$, and $\Gamma = \bigcap_{j \in \mathbb{N}_0} \Gamma_j$;*

(iii) **(sandwiched)** *$V := V(\Gamma) = \widetilde{H}^{-1/2}(\Gamma)$ and $V_j = V(\Gamma_j) = \widetilde{H}^{-1/2}(\Gamma_j)$, where Γ and Γ_j are non-empty, bounded and open with $\widetilde{H}^{-1/2}(\Gamma) = H_{\overline{\Gamma}}^{-1/2}$, and there exist Γ_j^- non-empty, bounded and open and Γ_j^+ non-empty and compact such that: $\Gamma_j^- \subset \Gamma_{j+1}^-$, $j \in \mathbb{N}_0$; $\Gamma_j^+ \supset \Gamma_{j+1}^+$, $j \in \mathbb{N}_0$; $\Gamma_j^- \subset \Gamma_j \subset \Gamma_j^+$, $j \in \mathbb{N}_0$; $\Gamma = \bigcup_{j \in \mathbb{N}_0} \Gamma_j^-$; $\overline{\Gamma} = \bigcap_{j \in \mathbb{N}_0} \Gamma_j^+$.*

Remark 4.4. *By combining Theorem 4.1 with Proposition 4.3 (i)-(ii) we reproduce the convergence results of [24, Thm. 7.1] (these phrased without reference to Mosco convergence). The convergence result obtained by combining Theorem 4.1 with Proposition 4.3 (iii), that applies in more subtle cases where neither $\Gamma_j \subset \Gamma$ nor $\overline{\Gamma} \subset \overline{\Gamma_j}$, is new. We present an example of this type (the "square snowflake") in §6.5 below.*

Remark 4.5. *The sequences $\Gamma_j^\pm$ required in Proposition 4.3(iii) exist if and only if*

$$\bigcap_{j \in \mathbb{N}_0} \Lambda_j^+ = \overline{\Gamma} \text{ and } \bigcup_{j \in \mathbb{N}_0} \Lambda_j^- = \Gamma, \text{ where } \Lambda_j^+ := \overline{\Gamma \cup \bigcup_{i=j}^\infty \Gamma_i} \text{ and } \Lambda_j^- := \Gamma \cap \left(\bigcap_{i=j}^\infty \Gamma_i\right)^\circ; \tag{30}$$

indeed if (30) holds then we can take $\Gamma_j^\pm := \Lambda_j^\pm$.

While parts (i) and (iii) of Proposition 4.3, and their BEM versions in Proposition 5.2 below, apply to more general bounded open screens Γ, we are particularly interested in cases where Γ has fractal boundary. The main challenge in applying part (iii) in such cases is to show that $\widetilde{H}^{-1/2}(\Gamma) = H_{\overline{\Gamma}}^{-1/2}$. But, as noted in Proposition 3.4, this holds if Γ is "thick" in the sense of Triebel, as recently shown in [15]. Moreover, it follows from [15, Prop. 5.1] that a large class of domains with fractal boundaries are thick. We provide some examples in §6 and §7.

4.1 Fractals that are attractors of iterated function systems

While Proposition 4.3 (ii), and its BEM version in Proposition 5.3 below, apply to more general compact Γ, our main motivation for these results is the case when Γ is fractal. An important fractal class (e.g. [33, Chap. 9]) is the set of fractals obtained as attractors of an iterated function system (IFS) $\{s_1, s_2, \ldots, s_\nu\}$. Here $\nu \geq 2$ and each $s_m : \mathbb{R}^{n-1} \to \mathbb{R}^{n-1}$ is a *contraction*, meaning that

$$|s_m(x) - s_m(y)| \leq c|x - y|, \quad x, y \in \mathbb{R}^{n-1},$$

for some $c \in (0, 1)$. The attractor of the IFS is the unique non-empty compact set Γ satisfying

$$\Gamma = s(\Gamma), \quad \text{where} \quad s(U) := \bigcup_{m=1}^{\nu} s_m(U), \quad \text{for } U \subset \mathbb{R}^{n-1}. \tag{31}$$

That (31) has a unique fixed point follows from the contraction mapping theorem since s is a contraction on the set of compact subsets of $\mathbb{R}^{n-1}$, a complete metric space equipped with the standard Hausdorff metric, e.g. [33, Thm. 9.1 and its proof]. If Γ_0 is any non-empty compact set then the sequence Γ_j defined by

$$\Gamma_{j+1} := s(\Gamma_j), \quad j = 0, 1, \ldots \tag{32}$$

converges in the Hausdorff metric to Γ. In particular, if Γ_0 is such that $s(\Gamma_0) \subset \Gamma_0$ then [33, Thm. 9.1]

$$\Gamma_{j+1} \subset \Gamma_j, \quad j \in \mathbb{N}_0, \quad \text{and} \quad \Gamma = \bigcap_{j \in \mathbb{N}_0} \Gamma_j. \tag{33}$$

In the case that Γ is a fractal or where Γ is not fractal but has a fractal boundary it is common to refer to Γ_j as a sequence of *prefractals*.

The following is an obvious corollary of the above observations, Theorem 4.1, and Proposition 4.3(ii).

Corollary 4.6. *Suppose that $\nu \geq 2$, $s_1, \ldots, s_\nu$ are contractions, and that the non-empty compact set $\Gamma \subset \Gamma_\infty \cong \mathbb{R}^{n-1}$ is the unique attractor of the IFS $\{s_1, \ldots, s_\nu\}$, satisfying (31). Suppose that Γ_0 is non-empty and compact with $s(\Gamma_0) \subset \Gamma_0$, and define the sequence of compact sets Γ_j by (32). Then BVP convergence holds.*

Remark 4.7. *With Γ_j defined by (32), it holds for any non-empty compact Γ_0 that $\Gamma_j \to \Gamma$ in the Hausdorff metric. However, if $s(\Gamma_0) \not\subset \Gamma_0$ it may or may not hold that $\phi_j \to \phi$ as $j \to \infty$. In particular, if: i) Γ_0 is a countable set; or ii) $n = 3$ and $\dim_H \Gamma_0 < 1$; then Γ_j defined by (32) is also countable or has $\dim_H \Gamma_j < 1$, respectively. (The latter case is a consequence of [33, Prop. 2.3].) In such cases it follows from Lemma 3.13 that $H_{\Gamma_j}^{-1/2} = \{0\}$ so that $\phi_j = 0$, for $j \in \mathbb{N}_0$. Thus $\phi_j \not\to \phi$ unless $\phi = 0$.*

5 Boundary element methods and their convergence

In this section we propose Galerkin boundary element methods, based on piecewise constant approximations, for solving the screen scattering problems of §3 and prove their convergence. These methods are based on discretisation of a sequence of more regular screens $(\Gamma_j)_{j\in\mathbb{N}_0}$; as in the previous section these converge in an appropriate sense to a limiting screen $\Gamma \subset \Gamma_\infty$ for which we wish to compute the solution to the scattering problem $D(\Gamma)$ of Definition 3.5 or 3.8.

In particular we have in mind cases where Γ is a compact set with fractal dimension $< n-1$, and cases where Γ is a bounded open set with fractal boundary. We prove convergence results that apply in both of these cases, and our examples in §6 and our numerical results in §7 are of these types. In each of our convergence results, Γ_j is a sequence of open sets, divided into a mesh of elements. Appropriately, given that we are approximating on very rough domains, the constraints on the elements are mild compared to conventional BEM results. In particular our elements need not be convex or even connected.

In more detail, we assume each Γ_j is a non-empty bounded open set. On each Γ_j we construct a *pre-convex mesh* $M_j = \{T_{j,1}, T_{j,2}, \ldots, T_{j,N_j}\}$ in the sense of Appendix A, meaning that $T_{j,l} \subset \Gamma_j$ is non-empty and open for $l = 1, \ldots, N_j$, the convex hulls of $T_{j,l}$ and $T_{j,l'}$ are disjoint for $l' \neq l$, $\partial T_{j,l}$ has zero $(n-1)$-dimensional Lebesgue measure, and Γ_j is the interior of the union of the closures of the $T_{j,l}$, i.e.

$$\Gamma_j = \left(\bigcup_{l=1}^{N_j} \overline{T_{j,l}} \right)^\circ.$$

We call $h_j := \max_{l\in\{1,\ldots,N_j\}} \operatorname{diam}(T_{j,l})$ the *mesh size* and $T_{j,1}, T_{j,2}, \ldots, T_{j,N_j}$ the *elements* of the mesh.

Our Galerkin boundary element method (BEM) is to solve the variational problem (29) with V_j chosen to be the N_j-dimensional space of piecewise constant functions on the mesh M_j, which we denote by V_j^h. It follows from (25), (26), and the comment following (9), that the BEM solution ϕ_j^h is defined explicitly by

$$(S_{\Gamma_j}^r \phi_j^h, \psi)_{L^2} = -(g_\dagger, \psi)_{L^2}, \quad \forall \psi \in V_j^h, \tag{34}$$

where $(\cdot, \cdot)_{L^2}$ is the inner product on $L^2 = L^2(\Gamma_\infty) = L^2(\mathbb{R}^{n-1})$. Moreover, when we are solving the scattering problem, $g_\dagger = -P_{\Gamma_\dagger} \gamma^\pm u^i$, and (34) can be written as

$$(S_{\Gamma_j}^r \phi_j^h, \psi)_{L^2} = (\gamma^\pm u^i, \psi)_{L^2}, \quad \forall \psi \in V_j^h.$$

Definition 5.1 (BEM convergence). *Let the discrete approximation space V_j^h be defined as above, and let the Sobolev space $V(\Gamma)$ be defined as in (23). If V_j^h Mosco-converges to $V(\Gamma)$ then we say that "BEM convergence holds". In this case, it follows by Theorem 4.1 that $\phi_j^h \to \phi$ in $H^{-1/2}$, where ϕ_j^h and ϕ are the solutions to (34) and (28), respectively, and $\mathcal{S}_{\Gamma_j} \phi_j^h \to \mathcal{S}_\Gamma \phi$ in $W^{1,\mathrm{loc}}(\mathbb{R}^n)$, with $\mathcal{S}_\Gamma \phi$ the solution to $\mathsf{D}(\Gamma)$ with $g = P_\Gamma g_\dagger$.*

5.1 Bounded open screens

The following theorem provides a BEM convergence result in the case where the limiting screen Γ is non-empty, bounded and open. The result is stated for case

(iii) in Proposition 4.3, but it also covers case (i), since if $\widetilde{H}^{-1/2}(\Gamma) = H_{\overline{\Gamma}}^{-1/2}$ (which we require in any case for well-posedness of $\mathsf{D}(\Gamma)$) then case (i) is a special case of case (iii) with $\Gamma_j^- = \Gamma_j$ and $\Gamma_j^+ = \overline{\Gamma}$, $j \in \mathbb{N}_0$.

Theorem 5.2 (Γ bounded and open). *Let Γ, Γ_j and $\Gamma_j^{\pm}$ satisfy the conditions of Proposition 4.3(iii). For each j, let M_j be a pre-convex mesh on Γ_j with mesh size h_j. Then BEM convergence holds provided that $h_j \to 0$ as $j \to \infty$.*

Proof. To show that $V_j^h \xrightarrow{M} V = \widetilde{H}^{-1/2}(\Gamma)$ we proceed by verifying that the conditions (i) and (ii) in Lemma 2.4 hold (with $W_j = V_j^h$, $W = V$, and $H = \widetilde{H}^{-1/2}(\Gamma_0^+)$). Regarding condition (ii), note that $V_j^h \subset \widetilde{H}^{-1/2}(\Gamma_j)$, and $\widetilde{H}^{-1/2}(\Gamma_j) \xrightarrow{M} \widetilde{H}^{-1/2}(\Gamma) = V$ by Proposition 4.3(iii). Regarding condition (i), let $v \in C_0^\infty(\Gamma)$ (which is dense in $V = \widetilde{H}^{-1/2}(\Gamma)$ by definition of the latter) be given. Since $\Gamma = \bigcup_{j \in \mathbb{N}_0} \Gamma_j^-$ and $\Gamma_j^- \subset \Gamma_{j+1}^-$ for $j \in \mathbb{N}_0$, it follows (e.g. [21, Lem. 4.15]) that there exists $j_* \in \mathbb{N}$ such that $\mathrm{supp}\, v \subset \Gamma_{j_*}^- \subset \Gamma_{j_*}$, and hence that $v \in C_0^\infty(\Gamma_j) \subset \widetilde{H}^{-1/2}(\Gamma_j)$, for all $j \geq j_*$. In particular, $v|_{\Gamma_j} \in L^2(\Gamma_j)$, so that by Lemma A.1

$$\|v - v_j\|_{\widetilde{H}^{-1/2}(\Gamma)} = \|v - v_j\|_{\widetilde{H}^{-1/2}(\Gamma_j)} \leq (h_j/\pi)^{1/2}\|v|_{\Gamma_j}\|_{L^2(\Gamma_j)}, \quad j \geq j_*,$$

where $v_j \in V_j^h$ is the L^2 projection of v onto the discrete space V_j^h. But since for $j \geq j_*$ the norm $\|v|_{\Gamma_j}\|_{L^2(\Gamma_j)} = \|v|_{\Gamma_{j_*}}\|_{L^2(\Gamma_{j_*})}$ does not depend on j, it follows that $v_j \to v$ provided $h_j \to 0$. $\qquad\square$

5.2 Compact screens

When the limiting screen Γ is compact and $\widetilde{H}^{-1/2}(\Gamma^\circ) \neq H_{\Gamma}^{-1/2}$, neither Theorem 5.2 nor its method of analysis can be applied. In particular, if $H_{\Gamma}^{-1/2} \neq \{0\}$ and Γ has empty interior ($\Gamma^\circ = \emptyset$) then it is clearly impossible to approximate a limiting non-trivial integral equation solution $v \in H_{\Gamma}^{-1/2}$ by a sequence of elements of $C_0^\infty(\mathbb{R}^{n-1})$ supported inside Γ, since no such non-trivial functions exist. In the following theorem we address this case. The proof relies on mollification arguments (see Appendix B) to obtain smooth approximations to v to which we can apply the BEM approximation theory (Lemma A.1). This produces approximating smooth functions whose support is strictly larger than that of v. This introduces a constraint on the sequence Γ_j to which the analysis applies. In particular, each Γ_j must contain $\Gamma(\epsilon) := \{\mathbf{x} \in \Gamma_\infty : \mathrm{dist}(\mathbf{x}, \Gamma) < \epsilon\}$, the ϵ-neighbourhood of Γ, for some carefully chosen j-dependent $\epsilon > 0$.

Theorem 5.3 (Γ compact). *Let $\Gamma \subset \Gamma_\infty$ be non-empty and compact. Let Γ_j be a sequence of bounded open subsets of Γ_∞ such that $\Gamma \subset \Gamma(\epsilon_j) \subset \Gamma_j \subset \Gamma(\eta_j)$, for some $0 < \epsilon_j < \eta_j$, with $\eta_j \to 0$ as $j \to \infty$. Let M_j be a pre-convex mesh on Γ_j with mesh size h_j. If H_Γ^t is dense in $H_\Gamma^{-1/2}$ for some $t \in [-1/2, 0]$ (always true for $t = -1/2$) then BEM convergence holds if $h_j = o((\epsilon_j)^{-2t})$ as $j \to \infty$.*

Proof. Assuming that $\eta_j \to 0$ as $j \to \infty$, to show that $V_j^h \xrightarrow{M} V = H_\Gamma^{-1/2}$ we proceed by verifying the two conditions (i) and (ii) in Lemma 2.4 (with $W_j = V_j^h$,

$W = V$, and $H = \widetilde{H}^{-1/2}(\Gamma_\dagger)$ for some bounded open set $\Gamma_\dagger \subset \Gamma^\infty$ that contains $\Gamma(\eta_j)$ for $j \in \mathbb{N}_0$). Regarding condition (ii) we note that $V_j^h \subset H_{\overline{\Gamma(\eta_j)}}^{-1/2}$, and $H_{\overline{\Gamma(\eta_j)}}^{-1/2} \xrightarrow{M} H_\Gamma^{-1/2} = V$ by Proposition 4.3(ii), since $\eta_j \to 0$. To establish condition (i), suppose that $v \in H_\Gamma^t$, where $t \in [-1/2, 0]$ is such that H_Γ^t is dense in $H_\Gamma^{-1/2}$. (Note that we are including $t = -1/2$ as a possibility here, in which case density holds trivially.) For each $j \in \mathbb{N}$ define $\tilde{v}_j := \psi_{\epsilon_j/2} * v$ to be the mollification defined in Appendix B. Then $\tilde{v}_j \in C_0^\infty(\Gamma_j)$ (since $\tilde{v}_j$ is smooth and supp $\tilde{v}_j \subset \overline{\Gamma(\epsilon_j/2)} \subset \Gamma(\epsilon_j) \subset \Gamma_j$) and $\|\tilde{v}_j - v\|_{H^{-1/2}(\Gamma_\infty)} \to 0$ as $j \to \infty$, since $\epsilon_j \to 0$. It remains to show that there exists $v_j \in V_j^h$ such that $\|v_j - \tilde{v}_j\|_{H^{-1/2}(\Gamma_\infty)} \to 0$ as $j \to \infty$. For this we define v_j to be the orthogonal projection in $L^2(\Gamma_j)$ of $\tilde{v}_j \in C_0^\infty(\Gamma_j)$ onto $V_j^h \subset L^2(\Gamma_j)$. From (47) we have that

$$\|\tilde{v}_j\|_{L^2(\Gamma_\infty)} \leq c_{n-1} c'_{-t}(\epsilon_j/2)^t \|v\|_{H_\Gamma^t},$$

so that, by Lemma A.1,

$$\begin{aligned}
\|v_j - \tilde{v}_j\|_{H^{-1/2}(\Gamma_\infty)} = \|v_j - \tilde{v}_j\|_{\widetilde{H}^{-1/2}(\Gamma_j)} &\leq (h_j/\pi)^{1/2} \|\tilde{v}_j\|_{L^2(\Gamma_j)} \\
&= (h_j/\pi)^{1/2} \|\tilde{v}_j\|_{L^2(\Gamma_\infty)} \\
&= c_{n-1} c'_{-t}(\epsilon_j/2)^t (h_j/\pi)^{1/2} \|v\|_{H_\Gamma^t}.
\end{aligned}$$

Hence $\|v_j - \tilde{v}_j\|_{H^{-1/2}(\Gamma_\infty)} \to 0$ as $j \to \infty$ provided that $h_j^{1/2} \epsilon_j^t \to 0$ as $j \to \infty$, which is equivalent to saying that $h_j = o(\epsilon_j^{-2t})$ as $j \to \infty$. $\qquad \square$

Remark 5.4. *Theorem 5.3 applies in the case when $V = H_\Gamma^{-1/2} = \{0\}$ when (trivially) $H_\Gamma^0 = \{0\}$ is dense in V, to give that $V_j^h \xrightarrow{M} V$ as $j \to \infty$, provided that $\eta_j \to 0$ and $h_j \to 0$ as $j \to \infty$. But, in this case, if $\eta_j \to 0$ then, as argued in the above proof, $V_j^h \subset H_{\overline{\Gamma(\eta_j)}}^{-1/2} \xrightarrow{M} V$ as $j \to \infty$, so that, by Lemma 2.4, $V_j^h \xrightarrow{M} V = \{0\}$ as $j \to \infty$, with no constraint on the mesh size h_j. More generally, if M_j is any mesh on any open set Γ_j such that $V_j = \widetilde{H}^{-1/2}(\Gamma_j) \xrightarrow{M} \{0\}$, then $V_j^h \xrightarrow{M} \{0\}$.*

Remark 5.5. *For many compact Γ of interest it is straightforward to see how to construct sequences Γ_j and M_j satisfying the conditions of Theorem 5.3 (see, for instance the examples in §6). But here is a construction that works in every case. Let $\mathcal{M}_1, \mathcal{M}_2, \ldots$ be a sequence of uniform meshes of convex elements on $\Gamma_\infty = \mathbb{R}^{n-1} \times \{0\}$, i.e. $\mathcal{M}_j = \{S_{j,n} : n \in \mathbb{N}\}$ is a family of open, bounded, convex, pairwise disjoint, congruent subsets of Γ_∞ that tile Γ_∞ in the sense that Γ_∞ is the closure of $\bigcup_{n=1}^\infty S_{j,n}$. Let h_j be the (common) diameter of $S_{j,n}$, for $n \in \mathbb{N}$, and assume that $h_j \to 0$ as $j \to \infty$. (For example, we might take (for $n = 2$) $\mathcal{M}_j = \{((n-1)h_j, nh_j) : n \in \mathbb{Z}\} \times \{0\}$.) For $j \in \mathbb{N}$ choose $\epsilon_j > 0$ with $\epsilon_j \to 0$ as $j \to \infty$, let M_j denote the set of those elements of $\mathcal{M}_j$ that have a non-empty intersection with $\Gamma(\epsilon_j)$, and let Γ_j denote the interior of $\overline{\bigcup_{T \in M_j} T}$, so that M_j is a convex mesh on Γ_j in the sense of §A (and, in particular, is pre-convex). Then $\Gamma(\epsilon_j) \subset \Gamma_j \subset \overline{\Gamma(\epsilon_j + h_j)} \subset \Gamma(\eta_j)$ provided $\eta_j > \epsilon_j + h_j$, so that Γ_j and M_j satisfy*

the conditions of Theorem 5.3 provided that $h_j = o(\epsilon_j^{-2t})$ for some $t \in [-1/2, 0]$ such that H_Γ^t is dense in $H_\Gamma^{-1/2}$.

Combining Theorem 5.3 and Remark 5.4 with the density results in Lemma 3.13 we obtain the following corollary.

Corollary 5.6. *Suppose that $\Gamma \subset \Gamma_\infty = \mathbb{R}^{n-1} \times \{0\}$, V, Γ_j, V_j^h and M_j satisfy the assumptions of Theorem 5.3. Then BEM convergence holds if either*

(i) $\dim_H \Gamma < n - 2$ or Γ is a $(n-2)$-set (so that $V = \{0\}$);
(ii) Γ is a d-set for some $n - 2 < d < n - 1$ (so that $V \neq \{0\}$) and $h_j = o(\epsilon_j^\mu)$ as $j \to \infty$, for some $\mu > n - 1 - d$.

We emphasize that in Corollary 5.6(ii) it is possible (since $0 < n - 1 - d < 1$) to take $\mu < 1$, giving convergence when $h_j \sim \varepsilon_j$ or even $h_j \gg \epsilon_j$. See the discussion around (42) and after Corollary 5.8(b) below, where this result is applied.

5.3 The BEM on fractals and prefractals arising from iterated function systems

An important IFS subclass is where each s_m is a *contracting similarity*, i.e.

$$|s_m(x) - s_m(y)| = r_m |x - y|, \quad x, y \in \mathbb{R}^{n-1}, \tag{35}$$

for some $r_m \in (0, 1)$. In the case that the IFS additionally satisfies the standard *open set condition* [33, (9.11)], that there exists a non-empty bounded open set $O \subset \mathbb{R}^{n-1}$ such that

$$s(O) \subset O \quad \text{and} \quad s_m(O) \cap s_{m'}(O) = \emptyset, \quad m \neq m', \tag{36}$$

it is well known [72, Thm. 4.7] that Γ is a d-set, in particular that $\dim_H \Gamma = d$, where $d \in (0, n-1]$ is the unique solution of the equation

$$\sum_{m=1}^\nu r_m^d = 1. \tag{37}$$

Thus Corollary 5.6 applies to this important class of fractal examples.

Suppose that O satisfies the open set condition, and consider the sequence of compact sets Γ_j defined by (32) with $\Gamma_0 := \overline{O}$, i.e.

$$\Gamma_0 := \overline{O}, \quad \Gamma_{j+1} := s(\Gamma_j), \quad j = 0, 1, \ldots \tag{38}$$

so that $\Gamma_j = s^j(\overline{O})$, where s^j is the mapping s iterated j times. Then the open set condition implies that $s(\overline{O}) \subset \overline{O}$, so that (33) holds, in particular $\Gamma \subset \overline{O}$, and it follows from Corollary 4.6 that the solution to the BVP $\mathsf{D}(\Gamma_j)$ converges to that of $\mathsf{D}(\Gamma)$ as $j \to \infty$. Note also that $s(O)$ has Lebesgue measure $|s(O)| = \sum_{m=1}^\nu r_m^{n-1} |O|$, so it follows from (37) that $d < n - 1$ unless $|s(O)| = |O|$, in which case $s(\overline{O}) = \overline{O}$ so that $\Gamma = \overline{O}$ (as Γ is the unique fixed point).

Furthermore, for any O satisfying the open set condition, the sequence Γ_j (cf. (38)) given by

$$\Gamma_0 := O, \quad \Gamma_{j+1} := s(\Gamma_j), \quad j = 0, 1, \ldots \tag{39}$$

so that $\Gamma_j = s^j(O)$, is a natural sequence of *open* sets converging to the fractal Γ that can be discretised by the BEM. For simplicity we assume for the rest of

this subsection that $r_m = r \in (0,1)$ for $m = 1, \ldots, \nu$ in (35), in which case (37) becomes

$$d = \log(r)/\log(1/\nu). \tag{40}$$

Assume that O is connected. Then the open set condition implies that Γ_j given by (39) has ν^j components, each component similar to O but reduced in diameter by a factor r^j. If O is convex and $M_0 = \{T_{0,1}, \ldots, T_{0,N_0}\}$ is a convex mesh on Γ_0, a natural construction of a convex mesh on Γ_j is to take

$$M_j := \left\{ s_{m_1} \circ \cdots \circ s_{m_j}\,(T_{0,l}) : 1 \leq m_{j'} \leq \nu \text{ for } j' = 1, \ldots, j \text{ and } 1 \leq l \leq N_0 \right\}. \tag{41}$$

The mesh M_j has N_0 elements on each component of Γ_j, so $N_j = \nu^j N_0$ elements in total. If h_0 is the mesh size for M_0, then M_j has mesh size $h_j = r^j h_0$.

One can also consider meshes for which there is less than one degree of freedom (DOF) per component of Γ_j. Precisely, for each j choose $i = i(j) \in \{0, \ldots, j\}$, let $\tau_{i,1}, \ldots, \tau_{i,\nu^i}$ be the components of Γ_i, and consider the mesh M_j on Γ_j defined by

$$M_j := \left\{ \Gamma_j \cap \tau_{i,1}, \ldots, \Gamma_j \cap \tau_{i,\nu^i} \right\}. \tag{42}$$

(Figure 1 shows the meshes given by (42) for $j = 0, 1, 2$ and $0 \leq i \leq j$ for a Cantor dust example from §6.2 below.) If $i = j$ the mesh (42) is convex (the elements are convex sets), indeed M_j coincides with the mesh given by (41) with $N_0 = 1$. But if $i < j$ then the mesh M_j given by (42) has only $N_j = \nu^i$ elements and each element is comprised of ν^{j-i} separate components. This mesh M_j is clearly not convex, if $i < j$, but it is pre-convex (in the sense of Appendix A) under the above assumptions on O, as captured in the following straightforward lemma.

Lemma 5.7. *Suppose that the bounded open set $O \subset \mathbb{R}^{n-1}$ is convex and satisfies the open set condition (36). Then M_j given by (42) is a pre-convex mesh on Γ_j.*

The following corollary, which follows from Theorems 4.1 and 5.3, Corollary 5.6 and Lemma 5.7, justifies convergence of the BEM when Γ_j is the sequence of prefractals (39) and M_j is defined by either (41) or (42), under the additional requirement that $\Gamma \subset O$ (rather than $\Gamma \subset \overline{O}$). We will see that this condition holds for obvious choices of O in the Cantor set and Cantor dust examples that we treat in the next sections.

Corollary 5.8. *Suppose that $\nu \geq 2$ and $s_1, \ldots, s_\nu$ are contracting similarities, satisfying (35) with $r_m = r$, for $m = 1, \ldots, \nu$ and some $r \in (0,1)$, and that the compact set Γ is the unique fixed point of the IFS $\{s_1, \ldots, s_\nu\}$, satisfying (31). Suppose that the bounded open set $O \subset \mathbb{R}^{n-1}$ is convex and satisfies the open set condition (36) and that $\Gamma \subset O$. Then Γ is a d-set with $d \in (0, n-1)$ given by (40).*

Define Γ_j by (39). Then BEM convergence holds if either

(a) M_j is the convex mesh defined by (41); or
(b) M_j is the pre-convex mesh defined by (42) and either
    (i) $d \leq n-2$ (so that $V = \{0\}$);
    (ii) $n-2 < d < n-1$ and $i(j) > \mu j$, $j \in \mathbb{N}_0$, for some $\mu > n-1-d$.

Proof. That Γ is a d-set with d given by (40) follows as discussed above; it holds, as discussed above (38), that $d < n-1$ since $\Gamma \subset O$ so that $\Gamma \neq \overline{O}$. Since O is bounded and open and $\Gamma \subset O = \Gamma_0$, it follows that $\Gamma \subset \Gamma(\epsilon_0) \subset \Gamma_0 \subset \Gamma(\eta_0)$, for some
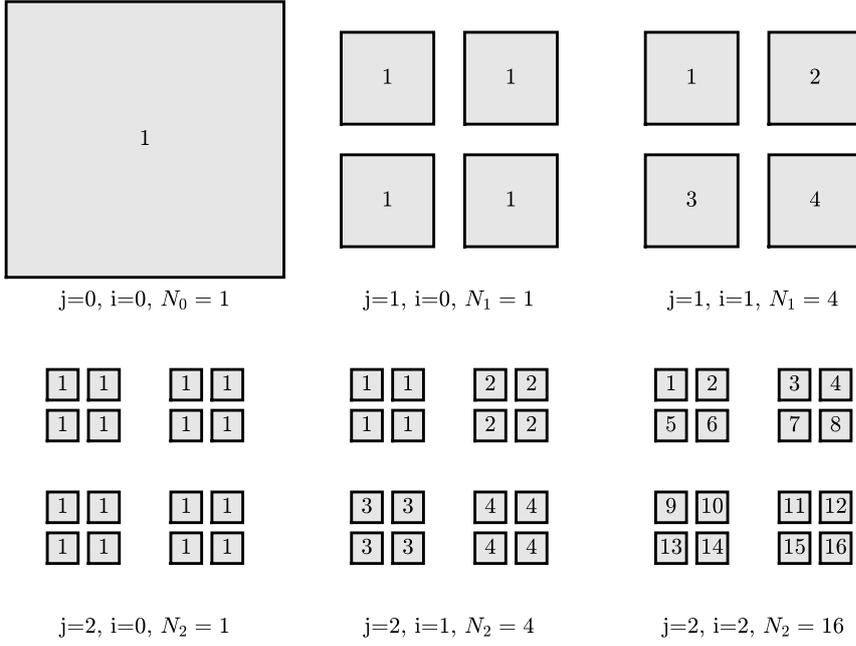
Fig. 1 Six pre-convex meshes, given by (42) with $j = 0, 1, 2$ and $i = 0, \ldots, j$, for the Cantor dust example of §6.2 with parameter $\alpha = 1/3$. The prefractals Γ_j are defined by (39) with $\Gamma_0 := O := (-\delta, 1 + \delta)^2$ and $\delta = 1/4$, and with $\nu = 4$ and the similarities $s_1, \ldots, s_\nu$ given by (43). Each mesh corresponds to a different pair of values (j, i). In each mesh the number inside each component of Γ_j is the index $\ell \in \{1, \ldots, N_j\}$ of the mesh element $\Gamma_j \cap \tau_{i,\ell}$ to which that component belongs, and $N_j = \nu^i$ is the total number of elements in the mesh on Γ_j.

$0 < \epsilon_0 < \eta_0$, so that, since $\Gamma = s^j(\Gamma)$ and $\Gamma_j = s^j(\Gamma_0)$, $\Gamma \subset \Gamma(\epsilon_j) \subset \Gamma_j \subset \Gamma(\eta_j)$, for $j \in \mathbb{N}_0$, with $\epsilon^j = r^j \epsilon_0$ and $\eta_j = r^j \eta_0$.

Suppose next that the mesh M_j on Γ_j is given by (41). Then the mesh size for M_j is $h_j = r^j h_0$, and that $V_j^h \xrightarrow{M} V$ as $j \to \infty$ follows from Corollary 5.6 applied with $\mu = 1$.

Suppose instead that M_j is given by (42) with $i = i(j) \in \{0, 1, \ldots, j\}$ and let L be the diameter of Γ_0. Then $h_j = r^i L$, and that $V_j^h \xrightarrow{M} V$ as $j \to \infty$ follows from Lemma 5.7 and Corollary 5.6, since, in the case $n - 2 < d < n - 1$, $i > \mu j$ for some $\mu > n - 1 - d$ implies that $h_j = o(\epsilon_j^\mu)$ as $j \to \infty$. $\square$

Corollary 5.8 proves BEM convergence for the case $\Gamma \subset O$ under rather mild mesh refinement. When $d \leq n - 2$ (zero limiting solution) there is no restriction on the mesh size, in accordance with Remark 5.4. When $n - 2 < d < n - 1$ (non-zero limiting solution) it is possible to take $\mu < 1$ in Corollary 5.8(ii)(b).[4] This means that BEM convergence holds with just one, or even less than one DOF per component of Γ_j.

---

[4] There is a curious "discontinuity in convergence" in Corollaries 5.6 and 5.8(ii): the infimum of the permitted μ values increases from 0 to 1 as d decreases from $n - 1$ to $n - 2$, then jumps back to 0 for $d < n - 2$.

Remark 5.9. *Corollary 5.8 does not apply to what is the standard choice of prefractal sequence in the Cantor set, Cantor dust, and Sierpinski triangle examples that we treat in §6, namely to define the sequence Γ_j by (39) with $O := (\mathrm{Conv}(\Gamma))^\circ$, the interior of the convex hull of Γ, which is an open interval, an open square, an open triangle, in the Cantor set, Cantor dust, and Sierpinski triangle cases, respectively. In each case this choice of O satisfies the open set condition, but it does not hold that $\Gamma \subset O$, only that $\Gamma \subset \overline{O}$.*

In such cases, assuming that $\widetilde{H}^{-1/2}(\Gamma_j) = H^{-1/2}_{\overline{\Gamma_j}}$ for each j, given an arbitrary element $v \in V = H^{-1/2}_{\Gamma}$ one can prove the existence of a sequence of mesh sizes h_j for which $\inf_{v_j^h \in V_j^h} \|v - v_j^h\|_{\widetilde{H}^{-1/2}} \to 0$ as $j \to \infty$ by a simple diagonal argument: since $V \subset V_j = \widetilde{H}^{-1/2}(\Gamma_j) = H^{-1/2}_{\overline{\Gamma_j}}$, there exists $v_j \in C_0^\infty(\Gamma_j)$ such that $\|v - v_j\|_{H^{-1/2}} \le (1+j)^{-1}$, say, and then by Lemma A.1 there exists h_j such that, if the mesh size on Γ_j is less than h_j, there exists $v_j^h \in V_j^h$ such that $\|v_j - v_j^h\|_{H^{-1/2}} \le (1+j)^{-1}$, and the claimed convergence follows by the triangle inequality. However, the required choice of h_j depends on v_j, which itself depends on v. So such an argument does not prove the existence of a single mesh refinement strategy for which $V_j^h \xrightarrow{M} V$.

The development of a satisfactory convergence analysis for BEM on these standard prefractal sequences remains an open problem.

6 Examples

We now apply the theory developed above to some specific examples of fractal screens. In our first example, the Cantor set, the scattering problem is posed in $\mathbb{R}^2$ (so $n = 2$), the screen being a subset of the one-dimensional hyperplane $\Gamma_\infty = \mathbb{R} \times \{0\}$. In all other examples, the scattering problem is posed in $\mathbb{R}^3$ (so $n = 3$), the screen being a subset of the two-dimensional hyperplane $\Gamma_\infty = \mathbb{R}^2 \times \{0\}$. In the first three examples Γ is a compact fractal d-set (for some $d < n - 1$) that is the attractor (31) of some IFS of contracting similarities $\{s_1, \ldots, s_\nu\}$. In the remaining examples Γ is a (relatively) open subset of Γ_∞ with fractal boundary.

6.1 Cantor sets

We consider first the Cantor set Γ, a compact subset of $\mathbb{R}$ with empty interior, depending on a parameter $0 < \alpha < 1/2$, defined by (31) with $\nu = 2$ and

$$s_1(x_1) = \alpha x_1, \quad s_2(x_1) = \alpha x_1 + 1 - \alpha.$$

Since the open set condition (36) holds with $O = (0, 1)$, Γ is a d-set with Hausdorff dimension $d = \log 2 / \log(1/\alpha)$. The standard prefractals Γ_j are defined by (32) with $\Gamma_0 := \overline{O} = [0, 1]$, so that Γ_j is the union of 2^j closed intervals of length α^j, and the Γ_j are a decreasing nested sequence of compact sets satisfying (33). To construct what we will term "thickened" open prefractals satisfying the conditions of Theorem 5.3, choose a parameter $0 < \delta < \frac{1}{2\alpha} - 1$, and define Γ_j by (39) with $\Gamma_0 := O := (-\delta, 1 + \delta)$, so that Γ_j is the disjoint union of the 2^j intervals of length $\alpha^j(1 + 2\delta)$ centred at the centres of the 2^j components of the standard prefractals.

Then $\Gamma \subset \Gamma(\epsilon_j) \subset \Gamma_j \subset \Gamma(\eta_j)$, for $\epsilon_j = \alpha^j \delta$ and for any $\eta_j > \sup_{x \in \Gamma_j} \mathrm{dist}(x, \Gamma) = \alpha^j \max\{\delta, 1/2 - \alpha\}$. Clearly we can choose η_j so that $\eta_j = O(\alpha^j) \to 0$ as $j \to \infty$.

The following result follows from Proposition 3.12, Lemma 3.13, Remark 5.4, Corollary 5.6, and Corollary 5.8.

Proposition 6.1 (Cantor set). *For $0 < \alpha < 1/2$, let Γ be the Cantor set defined above and let Γ_j be either the standard compact prefractals or the thickened open prefractals. Then the BVPs $\mathsf{D}(\Gamma)$ and $\mathsf{D}(\Gamma_j)$ are well-posed, BVP convergence holds, and the solution of $\mathsf{D}(\Gamma)$ is non-zero if and only if $g \neq 0$.*

For the thickened prefractals, BEM convergence holds if $h_j = o(\alpha^{\mu j})$ for some $\mu > \mu_0 := 1 - \frac{\log 2}{\log(1/\alpha)}$. In particular, BEM convergence holds for the convex mesh (41), and for the pre-convex mesh (42) with $i(j) > \mu j$, $j \in \mathbb{N}_0$, provided $\mu > \mu_0$.

Interpreted in terms of DOFs, the final statement in Proposition 6.1 says that BEM convergence holds for the pre-convex mesh (42) on the thickened prefractal Γ_j using $(2^{1 - \frac{\log 2}{\log 1/\alpha} + \epsilon})^j$ DOFs, for arbitrary $\epsilon > 0$. For example, for the middle third Cantor set ($\alpha = 1/3$) it suffices to take 1.3^j DOFs on Γ_j (note that Γ_j has 2^j components).

6.2 Cantor dusts

We now consider the Cantor dust Γ, a compact subset of $\mathbb{R}^2$ with empty interior, defined for $0 < \alpha < 1/2$ to be the Cartesian product of two identical Cantor sets from §6.1. Equivalently, the set Γ is defined by (31) with $\nu = 4$ and

$$s_1(x_1, x_2) = \alpha(x_1, x_2), \qquad\qquad s_2(x_1, x_2) = \alpha(x_1, x_2) + (1 - \alpha)(1, 0),$$
$$s_3(x_1, x_2) = \alpha(x_1, x_2) + (1 - \alpha)(0, 1), \quad s_4(x_1, x_2) = \alpha(x_1, x_2) + (1 - \alpha)(1, 1). \tag{43}$$

Since the open set condition (36) holds with $O = (0, 1)^2$, Γ is a d-set with Hausdorff dimension $d = \log 4 / \log(1/\alpha)$. The standard prefractals Γ_j are defined by (32) with $\Gamma_0 := \overline{O} = [0, 1]^2$, so that Γ_j is the union of 4^j closed squares of side length α^j, and the Γ_j are a decreasing nested sequence of compact sets satisfying (33). See Figure 2 for an illustration.
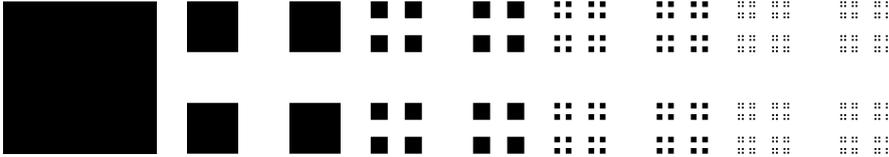
Fig. 2 The first five standard prefractals $\Gamma_0, \ldots, \Gamma_4$ of the middle third Cantor dust ($\alpha = 1/3$).

Thickened open prefractals satisfying the conditions of Theorem 5.3 can be constructed by taking Cartesian products of the thickened prefractals for the Cantor set. Explicitly, given $0 < \delta < \frac{1}{2\alpha} - 1$ we define Γ_j by (39) with $\Gamma_0 := O := (-\delta, 1 + \delta)^2$, so that Γ_j is the disjoint union of the 4^j squares of side length $\alpha^j(1 + 2\delta)$ centred at the centres of the 4^j components of the standard prefractals.

(Figure 1 shows (meshes on) Γ_0, Γ_1, and Γ_2 when $\alpha = 1/3$ and $\delta = 1/4$.) Then $\Gamma \subset \Gamma(\epsilon_j) \subset \Gamma_j \subset \Gamma(\eta_j)$, for $\epsilon_j = \alpha^j \delta$ and for any $\eta_j > \sup_{x \in \Gamma_j} \mathrm{dist}(x, \Gamma) = \sqrt{2}\alpha^j \max\{\delta, 1/2 - \alpha\} \to 0$ as $j \to \infty$.

The following result (cf. Proposition 6.1) follows from Proposition 3.12, Lemma 3.13, Remark 5.4, Corollary 5.6, and Corollary 5.8.

Proposition 6.2 (Cantor dust). *For $0 < \alpha < 1/2$, let Γ be the Cantor dust defined above and let Γ_j be either the standard compact prefractals or the thickened open prefractals. Then the BVPs $\mathsf{D}(\Gamma)$ and $\mathsf{D}(\Gamma_j)$ are well-posed, and BVP convergence holds.*

Now let Γ_j be either the interior of the standard compact prefractals, or the thickened open prefractals. Then

  (i) *for $0 < \alpha \le 1/4$, the solution of $\mathsf{D}(\Gamma)$ is zero, and BEM convergence holds for any pre-convex mesh on Γ_j;*
  (ii) *for $1/4 < \alpha < 1/2$, the solution of $\mathsf{D}(\Gamma)$ is non-zero if and only if $g \ne 0$, and BEM convergence holds for the thickened prefractals if $h_j = o(\alpha^{\mu j})$ for some $\mu > \mu_0 := 2 - \frac{\log 4}{\log(1/\alpha)}$. In particular, BEM convergence holds for the convex mesh defined by (41), and the pre-convex mesh defined by (42) with $i(j) > \mu j$, $j \in \mathbb{N}_0$, and $\mu > \mu_0$.*

Recalling Proposition 3.12, and comparing Propositions 6.1 and 6.2, we see that (provided the incident field doesn't vanish on the fractal screen), Cantor sets ($n = 2$) give rise to non-zero scattered fields for any value of α, while Cantor dusts ($n = 3$) give rise to non-zero scattered fields only for $\alpha > 1/4$.

6.3 Sierpinski triangle

The Sierpinski triangle (or gasket) Γ is a compact subset of $\mathbb{R}^2$ with empty interior, defined by (31) with $\nu = 3$ and

$$s_1(x_1, x_2) = \tfrac{1}{2}(x_1, x_2), \qquad\qquad s_2(x_1, x_2) = \tfrac{1}{2}(x_1, x_2) + (\tfrac{1}{2}, 0),$$
$$s_3(x_1, x_2) = \tfrac{1}{2}(x_1, x_2) + (\tfrac{1}{4}, \tfrac{\sqrt{3}}{4}).$$

Since the open set condition (36) holds with O the open unit equilateral triangle with vertices $(0, 0)$, $(1, 0)$, $(1/2, \sqrt{3}/2)$, Γ is a d-set with Hausdorff dimension $d = \log 3 / \log 2$. The standard prefractals Γ_j are defined by (32) with $\Gamma_0 := \overline{O}$ (the closed unit equilaterateral triangle), so that Γ_j is the (non-disjoint) union of 3^j closed equilateral triangles of side length 2^{-j}, and the Γ_j are a decreasing nested sequence of compact sets satisfying (33). The first five prefractals are shown in Figure 3.
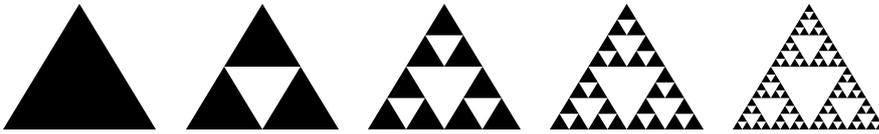
Fig. 3 The first five standard prefractals $\Gamma_0, \ldots, \Gamma_4$ of the Sierpinski triangle.

The interior Γ_j° of each prefractal is C^0 except at a finite set of points (the intersection points between neighbouring triangles), and hence by the results of §3 (see in particular Remark 3.11), the problems $\mathsf{D}(\Gamma_j)$ and $\mathsf{D}(\Gamma_j^\circ)$ share the same unique solution. To define thickened open prefractals satisfying the conditions of Theorem 5.3, given $\delta > 0$ we define O to be the open triangle of side length $1 + 2\delta$ with the same centre and side alignment as the unit equilateral triangle considered above, and define Γ_j by (39) with $\Gamma_0 := O$, so that Γ_j is the (non-disjoint) union of 3^j equilateral triangles of side length $2^{-j}(1 + 2\delta)$. Then $\Gamma \subset \Gamma(\epsilon_j) \subset \Gamma_j \subset \Gamma(\eta_j)$, for $\epsilon_j = 2^{-j}\delta/\sqrt{3}$ and for any $\eta_j > \sup_{x \in \Gamma_j} \mathrm{dist}(x, \Gamma) = (2^{-j+1}/\sqrt{3}) \max\{\delta, 1/4\} \to 0$ as $j \to \infty$.

For this choice of O, BEM convergence again follows from Theorem 5.3. But Corollary 5.8 does not apply here, because O does not satisfy the open set condition (disjointness fails). In fact, it is easy to see that for the Sierpinksi triangle there does not exist an open set O satisfying both the open set condition and the additional requirement that $\Gamma \subset O$.

Proposition 6.3 (Sierpinski triangle). *Let Γ be the Sierpinski triangle defined above and let Γ_j be either the standard compact prefractals or the thickened open prefractals. Then the BVPs $\mathsf{D}(\Gamma)$ and $\mathsf{D}(\Gamma_j)$ are well-posed, BVP convergence holds, and the solution of $\mathsf{D}(\Gamma)$ is non-zero if and only if $g \neq 0$.*

For the thickened prefractals, BEM convergence holds if $h_j = o(2^{-\mu j})$ for some $\mu > 2 - \frac{\log 3}{\log 2}$, in particular if $h_j = O(2^{-j})$.

6.4 Classical snowflakes

We now consider the family of "classical snowflakes" studied in [17], which generalise the standard Koch snowflake. Each snowflake Γ is a bounded open subset of $\mathbb{R}^2$ with fractal boundary, depending on a parameter $0 < \beta < \frac{\pi}{2}$, or equivalently on $\frac{1}{4} < \xi := \frac{1}{2(1 + \sin\beta)} < \frac{1}{2}$. The standard Koch snowflake corresponds to the choice $\beta = \pi/6$ ($\xi = 1/3$). We note that ξ is denoted α^{-1} in [17, §2]; our notation follows that in [15].

To define and approximate Γ we introduce a sequence of increasing nested open "inner prefractals" $(\Gamma_j^-)_{j \in \mathbb{N}_0}$, defining Γ by $\Gamma := \bigcup_{j \in \mathbb{N}_0} \Gamma_j^-$, and a sequence of decreasing nested closed "outer prefractals" $(\Gamma_j^+)_{j \in \mathbb{N}_0}$, such that $\Gamma \subset \Gamma_j^+$, $j \in \mathbb{N}_0$. The inner and outer prefractals for three examples (including the standard Koch snowflake) are shown in Figure 4.

Each Γ_j^- is an open polygon with $M_j^- := 3 \cdot 4^j$ edges of length ξ^j. Γ_0^- is the equilateral triangle with vertices $(0, 0)$, $(1, 0)$, $(\frac{1}{2}, \frac{1}{2}\sqrt{3})$. For $j \in \mathbb{N}$, Γ_j^- is the union of Γ_{j-1}^- and M_{j-1}^- identical disjoint isosceles triangles (together with their bases) with base length $\xi^{j-1}(1 - 2\xi)$, side length ξ^j, height $\xi^{j-1}\sqrt{\xi - \frac{1}{4}}$, apex angle 2β, placed in such a way that the midpoint of the base of the kth such triangle coincides with the midpoint of the kth side of Γ_{j-1}^-, for $k = 1, \ldots, M_j^-$.

Our sequence of "outer prefractals" generalises those considered in [6] for the standard Koch snowflake. Each Γ_j^+ is a closed polygon with $M_j^+ := 6 \cdot 4^j$ edges of length $\xi^{j+\frac{1}{2}}$. Γ_0^+ is the convex hexagon obtained as union of Γ_0^- and the three isosceles closed triangles with base the three sides of Γ_0^-, respectively, and height
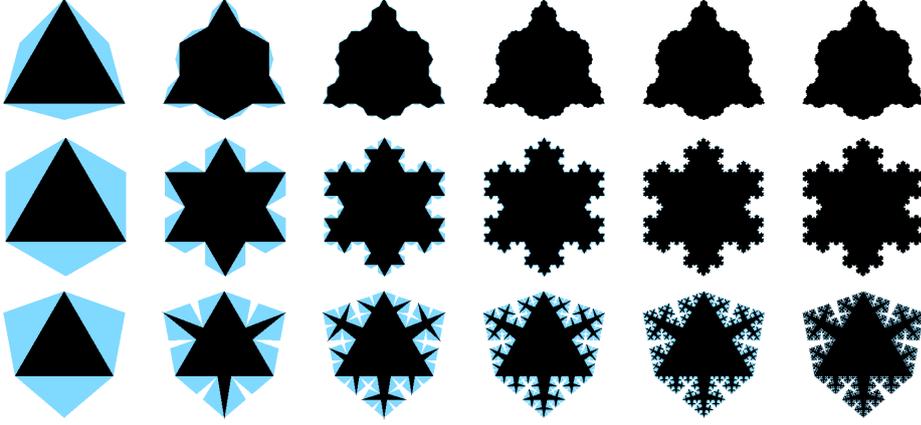
Fig. 4 The first 6 inner and outer prefractals $\Gamma_0^\pm, \ldots, \Gamma_5^\pm$ of the classical snowflakes for $\beta = \frac{\pi}{3}$ (top), $\beta = \frac{\pi}{6}$ (centre), $\beta = \frac{\pi}{20}$ (bottom). The inner prefractals Γ_j^- are the black shapes and the outer ones Γ_j^+ are the union of the blue and the black shapes. The parameter $0 < \beta < \frac{\pi}{2}$ represents half the width of each convex angle of the inner prefractals (except possibly the three angles of the first inner prefractal), and the parameter $1/4 < \xi = \frac{1}{2(1+\sin\beta)} < 1/2$ represents the ratio of the side lengths of two successive prefractals.

$\sqrt{\xi - \frac{1}{4}}$ (Γ_0^+ is a regular hexagon only if $\beta = \frac{\pi}{6}$). For $j \in \mathbb{N}$, Γ_j^+ is the difference of Γ_{j-1}^+ and M_{j-1}^+ identical disjoint isosceles triangles (together with their bases) with base length $\xi^{j-\frac{1}{2}}(1 - 2\xi)$, side length $\xi^{j+\frac{1}{2}}$, height $\xi^{j-\frac{1}{2}}\sqrt{\xi - \frac{1}{4}}$, apex angle 2β, placed in such a way that the midpoint of the base of the kth such triangle coincides with the midpoint of the kth side of Γ_{j-1}^+, for $k = 1, \ldots, M_j^+$.

Note that (cf. Figure 4) $\Gamma_j^- \subset \Gamma_j^+$, $\Gamma_j^- \subset \Gamma_{j+1}^-$ and $\Gamma_{j+1}^+ \subset \Gamma_j^+$ for each $j \in \mathbb{N}_0$.

In [15] we proved that

- $\overline{\Gamma} = \bigcap_{j \in \mathbb{N}_0} \Gamma_j^+$, $\Gamma = (\overline{\Gamma})^\circ$ and $|\partial\Gamma| = 0$;
- $\partial\Gamma$ is a d-set with Hausdorff dimension $d = \log 4/\log(1/\xi)$ (with the standard Koch snowflake having dimension $\log 4/\log 3$);
- Γ is a "thick" domain (in the sense of Triebel), so $\widetilde{H}^s(\Gamma) = H_{\overline{\Gamma}}^s$ for all $s \in \mathbb{R}$.

Combining these facts with Theorem 3.2, Proposition 3.7, Proposition 4.3(iii) and Theorem 5.2, gives the following result.

Proposition 6.4 (Classical snowflakes). *Let $0 < \beta < \frac{\pi}{2}$, and define the classical snowflake Γ and its inner and outer prefractals $\Gamma_j^\pm$ as above. Let Γ_j be any sequence of bounded open sets satisfying $\Gamma_j^- \subset \Gamma_j \subset \Gamma_j^+$, with $\widetilde{H}^{-1/2}(\Gamma_j) = H_{\overline{\Gamma_j}}^{-1/2}$ (in particular this applies if $\Gamma_j = \Gamma_j^-$ or $\Gamma_j = (\Gamma_j^+)^\circ$, since then Γ_j is C^0). Then the BVPs $\mathsf{D}(\Gamma)$ and $\mathsf{D}(\Gamma_j)$ are well-posed, and BVP convergence holds. Furthermore, BEM convergence holds if $h_j \to 0$ as $j \to \infty$.*

6.5 Square snowflake

As our final example we consider the "square snowflake" studied in [64] (see also [36, §7.6] and the references therein). This is an open subset of $\mathbb{R}^2$ with fractal boundary, constructed as the limit of a sequence of *non-nested* polygonal prefractals Γ_j, $j \in \mathbb{N}_0$, the first five of which are shown in Figure 5.
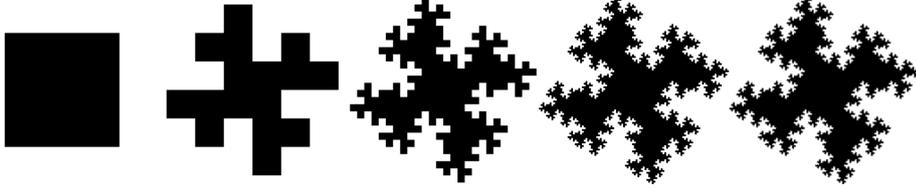
Fig. 5 The first five standard prefractals $\Gamma_0, \ldots, \Gamma_4$ of the square snowflake.

Each prefractal Γ_j is an open polygon whose boundary is the union of $N_j := 4 \cdot 8^j$ segments of length $\ell_j := 4^{-j}$ aligned to the Cartesian axes. Let $\Gamma_0 = (0,1)^2$ be the open unit square. For $j \in \mathbb{N}$, $\partial\Gamma_j$ is constructed by replacing each horizontal edge and each vertical edge of $\partial\Gamma_{j-1}$ respectively by the following polygonal lines composed of 8 edges each:
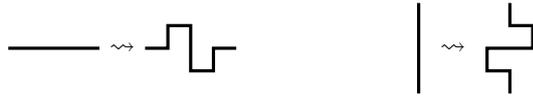
(Note that the fourth and the fifth segments obtained are aligned; in the following however we count them as two different edges of Γ_j.) Each polygonal path $\partial\Gamma_j$ constructed with this procedure is the boundary of a simply connected polygon Γ_j of unit area, composed of 16^j squares of side length ℓ_j. (See [15, §5.2] for more detail of this construction.) The resulting sequence of prefractals $\{\Gamma_j\}_{j \in \mathbb{N}_0}$ is not nested: for each $j \in \mathbb{N}$ neither $\Gamma_j \subset \Gamma_{j-1}$ nor $\Gamma_j \supset \Gamma_{j-1}$. Indeed, the two set differences $\Gamma_j \setminus \Gamma_{j-1}$ and $\Gamma_{j-1} \setminus \Gamma_j$ are composed of $4 \cdot 8^{j-1} = 2^{3j-1}$ disjoint squares of side length ℓ_j. Thus the limit set of the sequence cannot be defined simply as a union or intersection of the prefractals.

In [15] we showed how to construct inner and outer nested prefractal sequences $\Gamma_j^\pm$ such that Γ_j and $\Gamma_j^\pm$ satisfy the assumptions of Proposition 4.3(iii), with the limit set Γ defined as $\Gamma := \bigcup_{j \in \mathbb{N}_0} \Gamma_j^- = \left(\bigcap_{j \in \mathbb{N}_0} \Gamma_j^+\right)^\circ$. In [15] we proved further that $\partial\Gamma$ is a d-set with Hausdorff dimension $d = 3/2$, and that Γ is a thick domain, so that $\widetilde{H}^s(\Gamma) = H_{\overline{\Gamma}}^s$ for all $s \in \mathbb{R}$. Combining these facts with Theorem 3.2, Proposition 3.7, Proposition 4.3(iii) and Theorem 5.2, gives the following result.

Proposition 6.5 (Square snowflake)**.** *Define the square snowflake Γ and its standard prefractals Γ_j as above. Then the BVPs $\mathsf{D}(\Gamma)$ and $\mathsf{D}(\Gamma_j)$ are well-posed, and BVP convergence holds. Furthermore, BEM convergence holds if $h_j \to 0$.*

7 Numerical results

In this section we present numerical results validating our theory, and demonstrate the feasibility of using BEM to calculate scattering by fractal screens.

While our theoretical convergence analysis in §§5-6 is for Galerkin discretisations, the numerical results in this section were obtained using a collocation method, to make implementation as simple and flexible as possible. Our Matlab collocation code was validated against our own 2D Galerkin code for the case of the Cantor set (see Figure 8 below) and the open-source 3D Galerkin software Bempp [66] for the case of the Sierpinski triangle. In both cases, for fixed prefractal level the collocation code was found to give similar accuracy to the Galerkin codes (using the same meshes), but with a slightly lower computational cost, allowing us to reach slightly higher prefractal levels in 3D than was possible with the Galerkin code (using default Bempp settings and dense linear algebra).

All our experiments are on prefractals that are finite unions of disjoint segments (when $n = 2$) or finite unions of Lipschitz polygons (when $n = 3$). For simplicity we use uniform meshes throughout. In fact, in each experiment the elements are either congruent segments (when $n = 2$), or congruent squares, or congruent equilateral triangles.

7.1 Collocation method

Given a prefractal Γ_j partitioned by a uniform mesh $M_j = \{T_{j,1}, \ldots, T_{j,N_j}\}$ with mesh size h_j (the diameter of each element of the uniform mesh), our collocation discretisation of the BIE (21) computes $\phi_j^h \in V_j^h$ (the N_j-dimensional space of piecewise constants on M_j) by solving the equations

$$(S_{\Gamma_j} \phi_j^h)(\mathbf{x}_l) = -g_\dagger(\mathbf{x}_l), \qquad l = 1, \ldots, N_j,$$

where $\mathbf{x}_l$ is the centre of the element $T_{j,l}$. This is equivalent to approximating the testing integrals in the Galerkin equations (34) with a 1-point-per-element quadrature formula.

The vector $\mathbf{u}$ containing the values of ϕ_j^h on each mesh element satisfies a square linear system $A\mathbf{u} = \mathbf{b}$ where the matrix A and right-hand side vector $\mathbf{b}$ have entries $A_{l,m} = \int_{T_{j,m}} \Phi(\mathbf{x}_l, \mathbf{x}) \mathrm{d}s(\mathbf{x})$ and $b_l = -g_\dagger(\mathbf{x}_l)$, respectively. The integrals in the off-diagonal matrix entries are approximated with Gauss–Legendre quadrature on line segments and the tensorized version of the same rule on square elements; in both cases the number of quadrature points per element is chosen to be at least $\max\{20h_j/\lambda, 3\}^{n-1}$, $\lambda = 2\pi/k$ being the wavelength. Numerical tests show that higher-order quadratures do not noticeably improve solution accuracy for the range of parameters considered. On triangular elements we use a classical 7-point symmetric formula (as in [62, p. 415], with degree of exactness 3). The integrands of the diagonal entries $A_{l,l}$ have a weak singularity at the element centre $\mathbf{x}_l$. For line segments, $A_{l,l}$ is computed by dividing the segment in half and applying a high-order Gauss–Legendre quadrature on each side of the singularity. For square and equilateral triangle elements we split $T_{j,l}$ into 4 or 3 identical isosceles triangles respectively (with a common corner at the singularity), apply

symmetry, and transform to polar coordinates, to evaluate $A_{l,l}$ as

$$
A_{l,l} = \int_{T_{j,l}} \frac{\mathrm{e}^{\mathrm{i}k|\mathbf{x}-\mathbf{x}_l|}}{4\pi|\mathbf{x}-\mathbf{x}_l|}\mathrm{d}\mathbf{x} = \begin{cases} \dfrac{1}{\pi \mathrm{i}k} \displaystyle\int_{-\pi/4}^{\pi/4} (\mathrm{e}^{\frac{\mathrm{i}kL}{2\cos\theta}} - 1)\mathrm{d}\theta & \text{if } T_{j,l} \text{ is a square,} \\[2ex] \dfrac{3}{4\pi \mathrm{i}k} \displaystyle\int_{-\pi/3}^{\pi/3} (\mathrm{e}^{\frac{\mathrm{i}kL}{2\sqrt{3}\cos\theta}} - 1)\mathrm{d}\theta & \text{if } T_{j,l} \text{ is a triangle,} \end{cases}
$$

where L is the element side length. The integrals over θ are computed using Matlab's `integral` function. Since the mesh is uniform, all diagonal terms coincide and only one such computation is needed for a given value of kL. The (dense, complex, non-Hermitian) linear systems in our numerical experiments are relatively small (with fewer than 11000 DOFs) and are solved with a direct solver (Matlab's backslash).

7.2 Experiments performed

We use our BEM code to compare the numerical solutions on a sequence of prefractal screens Γ_j approximating a limiting fractal screen Γ, for the examples in §6. In addition to showing domain plots of the scattered fields for different Γ_j, we study the j-dependence of the norm of the numerical solution using the three norms defined in Table 1. The table also shows the marker type these norms will be represented by in all the plots. To validate our theoretical convergence results we also compute near- and far-field errors for the solution on Γ_j, relative to the solution on the finest prefractal $\Gamma_{j_{\max}}$, using these same norms. In all tests we simulate scattering problems, and the incident field is a plane wave, so that $g_{\dagger}(\mathbf{x}) = -\mathrm{e}^{\mathrm{i}k\mathbf{d}\cdot\mathbf{x}}$, $\mathbf{x} \in \Gamma_j$, for some $\mathbf{d} \in \mathbb{S}^{n-1}$, the incident wave direction. In the convergence plots for compact screens, red continuous lines correspond to results for standard prefractals and blue dashed lines to results for thickened prefractals.

7.3 Cantor set

We first fix Γ to be the standard Cantor set, as defined in §6.1, with $\alpha = 1/3$, set $k = 30$ (so that the acoustic wavelength $\lambda := 2\pi/k \approx 0.209$ and there are roughly 5 wavelengths across Γ), and choose the direction of the incident plane wave as $\mathbf{d} = (1/2, -\sqrt{3}/2)$.

We make BEM computations on both the standard (open) prefractals Γ_j, defined by (39) with $O = (0,1)$, which have 2^j components of length 3^{-j} (cf. §6.1), and the thickened prefractals as defined in §6.1 with $\delta = \frac{1}{4\alpha} - \frac{1}{2} = \frac{1}{4}$, which we denote by Γ_j^{δ}, and which have 2^j components of length $\frac{3}{2}3^{-j}$. We present results for the simplest case where the BEM meshes have exactly one element per component of each prefractal, so that we are using the convex mesh (41) with $N_0 = 1$. Thus there are $N_j = 2^j$ elements and DOFs on the jth prefractal. For these simple meshes (Galerkin) BEM convergence is guaranteed for the thickened prefractals by Proposition 6.1.

Figure 6 shows the real part and magnitude of the scattered and total fields on the box $(-1,2) \times (-1.5, 1.5)$, computed for prefractal level $j = 13$, discretising Γ_{13}^{δ} with $N_{13} = 2^{13} = 8192$ elements and DOFs.

Marker	Norm
○	The $\widetilde{H}^{-1/2}(\Gamma_j)$ norm on Γ_j, computed via an accurate numerical integration of the representation $\|\phi_j^h\|_{\widetilde{H}^{-1/2}(\Gamma_j)}^2 = 2\int_{\Gamma_j}(S_{\Gamma_j}^i\phi_j^h)\overline{\phi_j^h}\,\mathrm{d}s$, where $S_{\Gamma_j}^i$ is the single-layer operator for the equation $\Delta u - u = 0$ (compare the definition of the norm in §2.4 and [38, eq. (3.5), (3.28)]).
□	The $L^2(Box)$ norm in a near-field region, computed over the "box" used for the domain plots. For the Cantor set this "box" is the square $(-1,2)\times(-1.5,1.5)$. For all other examples it comprises three perpendicular faces of the cuboid $(-1,2)\times(-1,2)\times(-1,1)$. See e.g. Figures 6 and 10.
*	The $L^2(\mathbb{S}^{n-1})$ norm on $\mathbb{S}^{n-1} := \{\hat{\mathbf{x}} \in \mathbb{R}^n, |\hat{\mathbf{x}}| = 1\}$, the unit sphere. In particular we compute this quantity for the far-field pattern $u_{j,\infty}$ of the field scattered from Γ_j, defined by $u_{j,\infty}(\hat{\mathbf{x}}) := \frac{-\mathrm{i}k^{(n-3)/2}}{2(2\pi\mathrm{i})^{(n-1)/2}}\int_{\Gamma_j}\mathrm{e}^{-\mathrm{i}k\hat{\mathbf{x}}\cdot\mathbf{y}}\phi_j^h(\mathbf{y})\mathrm{d}s(\mathbf{y})$, for $\hat{\mathbf{x}} \in \mathbb{S}^{n-1}$ [29, (2.13), (3.64)]. This norm is proportional to the square root of the total acoustic power flux in the scattered field.

Table 1 The graphical conventions used in the plots.
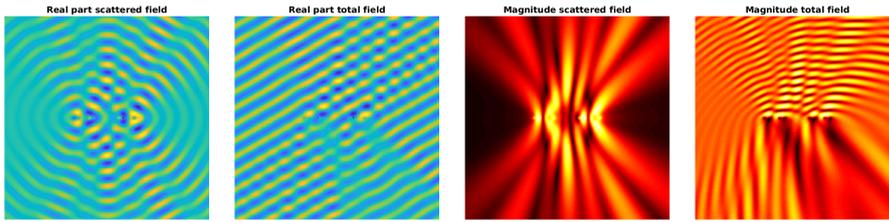
Fig. 6 The real part and magnitude of the scattered and total fields on the box $(-1,2)\times(-1.5,1.5)$ for the Cantor set problem in §7.3, approximating Γ by the level 13 thickened prefractal Γ_{13}^δ and using $N_{13} = 8192$ DOFs.

The left panel in Figure 7 shows the norms, as defined in Table 1, of the (collocation) BEM solution on Γ_j and Γ_j^δ for $j = 0, \ldots, 13$. In all cases the norms quickly settle to an approximately constant value, suggesting that a limiting value as $j \to \infty$ has been reached. The right panel in Figure 7 shows the near- and far-field relative errors for $j = 0, \ldots, 12$, measured against the solutions for $j = 13$. Standard prefractals seem to give slightly smaller errors than thickened ones. But in both cases the relative errors decay exponentially in j, this numerical evidence of collocation BEM convergence, both for standard and thickened prefractals.

For this specific 2D problem we have also implemented a Galerkin BEM. The left panel of Figure 8 demonstrates the close agreement between our collocation solutions and the corresponding Galerkin solution (to which Proposition 6.1 applies to prove convergence in the thickened prefractal case). Taken together, since we know from Proposition 6.1 that the Galerkin solution on the thickened prefractal sequence converges to the correct limiting solution of the BIE on the Cantor set
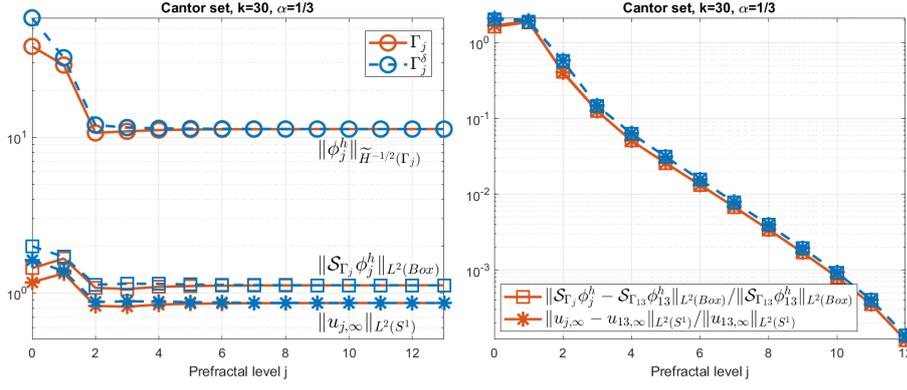
Fig. 7 Numerical results for the Cantor set problem in §7.3 for prefractal levels 0 to 13. Left: the convergence of the boundary, near- and far-field norms of the discrete solutions. Right: the exponential decay (in j) of the near- and far-field relative errors between the solutions on the jth prefractal and the 13th prefractal. Continuous red lines correspond to standard prefractals and dashed blue lines show the same quantities for thickened prefractals.
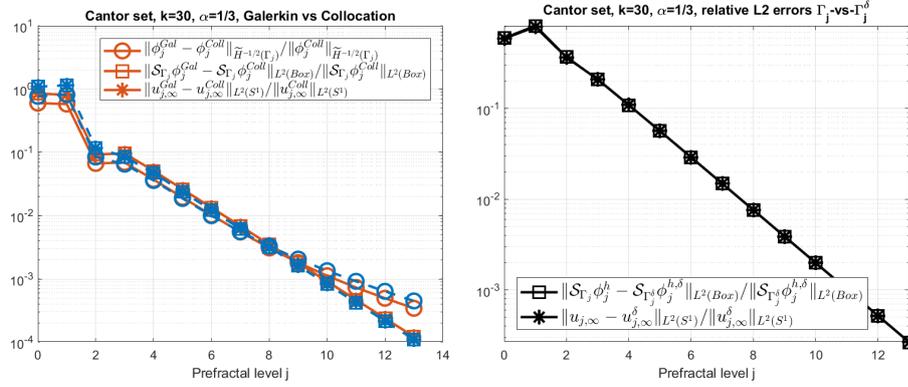
Fig. 8 Left: validation of our collocation code against a Galerkin implementation for the Cantor set problem in §7.3. Continuous red lines correspond to standard prefractals and dashed blue lines show the same quantities for thickened prefractals (see Table 1). Note that there are 6 lines in total on this graph, but the near-field and far-field relative errors are almost indistinguishable. Right: exponential decay of the relative difference between the fields scattered by the standard (Γ_j) and thickened (Γ_j^δ) prefractals for the Cantor set problem in §7.3. Here $\phi_j^{h,\delta}$ and $u_{j,\infty}^\delta$ denote the BEM solution on Γ_j^δ and the corresponding far-field pattern.

Γ, Figures 7 and 8 are persuasive numerical evidence that: i) the Galerkin solution on the standard prefractal sequence; and ii) the collocation solutions on both the standard and the thickened prefractal sequences, are all converging to the correct limiting solution for the Cantor set Γ as $j \to \infty$. These conclusions are further supported by the right panel in Figure 8 which shows that the near and far-field relative differences between the fields computed on the standard and thickened prefractals (using collocation BEM) also decrease exponentially in j.

Figure 9 shows how norms of the Cantor set solution, approximated by (collocation BEM) computations on the finest prefractal level, vary as a function of

the Cantor set parameter α. Recall that α is related to the Hausdorff dimension of the Cantor set Γ by $d = \log 2 / \log(1/\alpha)$. The strength of the scattered field decreases with decreasing α (decreasing d). This is consistent with our earlier theory. Specifically, let $(\alpha_\ell)_{\ell \in \mathbb{N}_0} \subset (0, 1/2)$ be any decreasing sequence such that $\alpha_\ell \to 0$, and let Γ_ℓ^C denote the corresponding sequence of Cantor sets, and let $\Gamma_\ell^{C,+} := \bigcup_{i \geq \ell} \Gamma_i^C$. Then, since $\Gamma_{\ell+1}^{C,+} \subset \Gamma_\ell^{C,+}$, it follows from Theorem 4.1 and Proposition 4.3(ii) that BVP convergence holds, specifically that the solution for $\Gamma_\ell^{C,+}$ converges to that for $\Gamma^C := \bigcap_{\ell \in \mathbb{N}_0} \Gamma_\ell^{C,+}$ as $\ell \to \infty$. But $\Gamma^C = \{0, 1\}$, since $\{0, 1\} \subset \Gamma_\ell^{C,+} \subset [0, \alpha_\ell] \cup [1 - \alpha_\ell, 1]$ for each ℓ. Thus, by Lemma 3.13 and Proposition 3.12, $H_{\Gamma^C}^{-1/2} = \{0\}$ and the field scattered by Γ^C is zero. Further, by Lemma 2.3, since $\Gamma_\ell^C \subset \Gamma_\ell^{C,+}$, the solution for Γ_ℓ^C also converges to zero as $\ell \to \infty$.
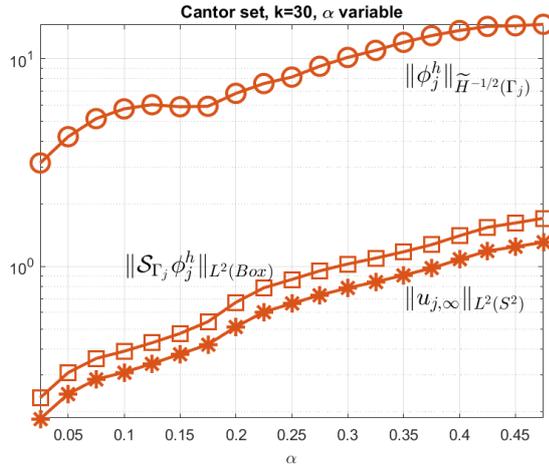
Fig. 9 Solution norms for the finest standard prefractal Γ_{13}, plotted against the Cantor set parameter α.

7.4 Cantor dust

We now make computations for two Cantor dusts, as defined in §6.2, with $\alpha = 1/3$ and $\alpha = 1/10$ respectively, setting $k = 50$ (so that $\lambda \approx 0.126$ and there are roughly 11 wavelengths across the diagonal of Γ), and choosing $\mathbf{d} = (0, \frac{1}{\sqrt{2}}, -\frac{1}{\sqrt{2}})$.

Similarly to §7.3 we make (collocation) BEM computations on both the standard (open) prefractals Γ_j, defined by (39) with $O = (0, 1)^2$ (cf. §6.2), and the thickened prefractals as defined in §6.2 with $\delta = \frac{1}{4}$, which we denote by Γ_j^δ. As in §7.3 we use BEM meshes with exactly one element per component of each prefractal, giving $N_j = 4^j$ DOFs in total. It follows from Proposition 6.2 that (Galerkin) BEM convergence is guaranteed for the standard prefractals for $\alpha = 1/10$ (since the limiting solution is zero), and for the thickened prefractals for both $\alpha = 1/3$ and $\alpha = 1/10$.
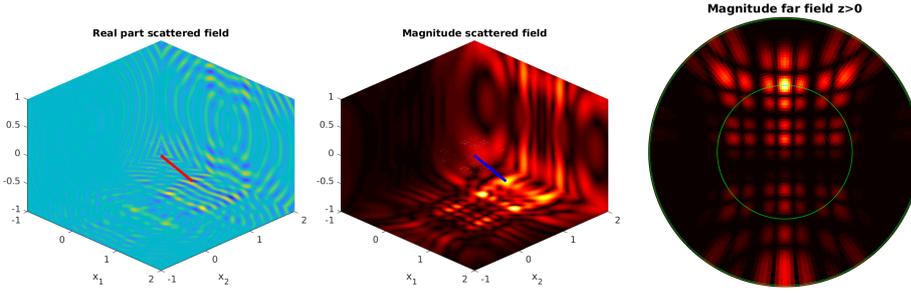
Fig. 10 The scattered field for the Cantor dust problem in §7.4 with $\alpha = 1/3$, computed on Γ_6 with $N_6 = 4096$ DOFs. Left and centre: the real part and magnitude of the scattered field on three faces of the box $(-1, 2) \times (-1, 2) \times (-1, 1)$ (with $\Gamma \subset (0, 1)^2 \times \{0\}$). The red/blue segment denotes the direction of the incoming wave. Right: the magnitude of the far-field pattern $u_{j,\infty}$ on the upper half-sphere $\mathbb{S}^2 \cap \{x_3 > 0\}$; the angular coordinate is the longitude, the radial coordinate the colatitude (the green circle through the bright spot is the $\pi/4$ parallel).

Figure 10 shows near- and far-field plots of the scattered field for the standard prefractal of level $j = 6$ with $N_6 = 4^6 = 4096$ DOFs.

Figure 11 shows the solution norms for prefractal levels 0 to 6 and the relative errors against the computations on the finest prefractal. From the left panels we see that for $\alpha = 1/3$ the norms appear to converge to a constant positive value, while for $\alpha = 1/10$ they converge (exponentially) to 0, consistent with Proposition 6.2. The superior convergence rate in the near- and far-field L^2 norms compared to the $\widetilde{H}^{-1/2}$ energy norm, visible for $\alpha = 1/10$, is in line with standard superconvergence theory for functionals of a BEM solution—see e.g. [67, §4.2.5].

In the right panels of Figure 11 we observe the exponential (in j) decay of the errors of near- and far-fields against the solutions on the finest prefractal. We have also computed (but do not plot) the differences between standard and thickened prefractals in the near- and far-fields. These behave similarly to those in Figure 8 (for $n = 2$). These various numerical experiments, together with validations we have made (see the beginning of §7) of our collocation code against 3D Galerkin code, and the theoretical (Galerkin) BEM convergence results of Proposition 6.2, provide persuasive evidence (cf. the penultimate paragraph of §7.3) that our collocation BEM results are converging as $j \to \infty$ to the correct limiting solution for scattering by the Cantor dust Γ.

The left panel of Figure 12 shows how the magnitude of the scattered field depends on the parameter α, and thus on the Hausdorff dimension $d = \log 4/\log(1/\alpha)$, for different prefractal levels j. Note that in this experiment we used a fixed total number $N_j = 4096$ of DOFs on each prefractal, so that the lower order prefractal solutions are computed more accurately than they would be using our usual prescription $N_j = 4^j$. We recall (Proposition 6.2) that in the limit $j \to \infty$ the field should vanish for $\alpha \leq 1/4$; compare this to the right panel of Figure 9 for the Cantor set ($n = 2$), where the limit is non-zero for all α.

The right panel of Figure 12 shows the dependence on the wavenumber k of $\|\phi_j^h\|_{\widetilde{H}^{-1/2}(\Gamma_j)}$, for the largest prefractal level $j = 6$ that approximates the fractal limit. We find that $\|\phi_6^h\|_{\widetilde{H}^{-1/2}(\Gamma_6)}$ grows with increasing k like $k^{0.19}$ for the larger values of k. In the same panel we also plot $\|\phi_6^h\|_{\widetilde{H}_k^{-1/2}(\Gamma_6)}$ and $\|\phi_0^h\|_{\widetilde{H}_k^{-1/2}(\Gamma_0)}$
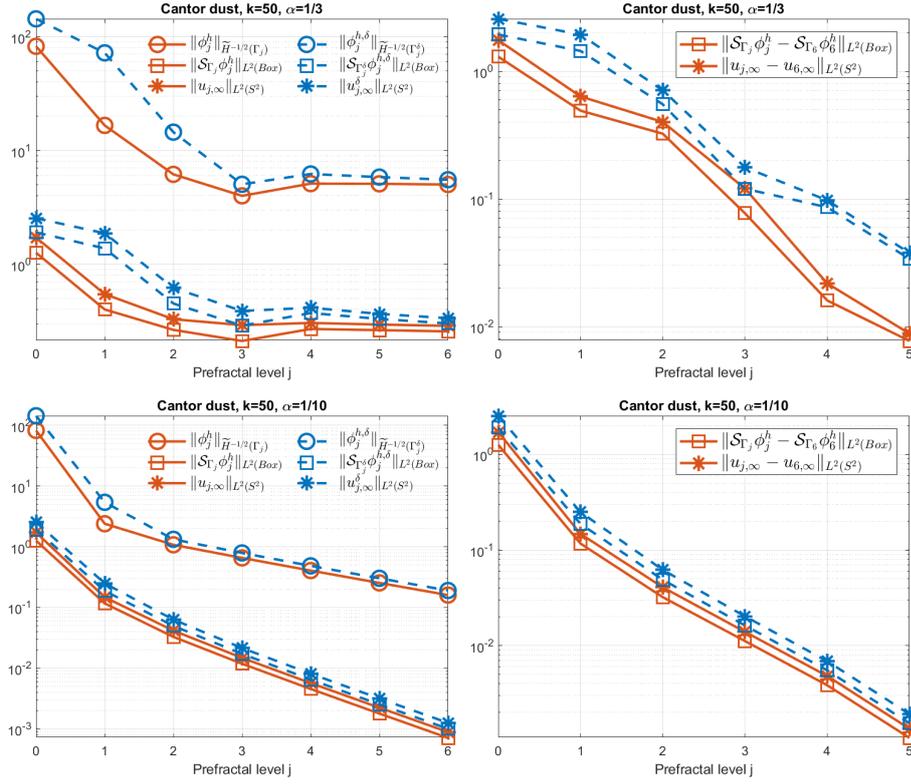
Fig. 11 Analogue of Figure 7 for the Cantor dust problem in §7.4, except that in the right column we show absolute errors. Top row: $\alpha = 1/3$, bottom row: $\alpha = 1/10$. From the left plots we see that, when the prefractal is refined, the solution norms converge to positive values for $\alpha = 1/3$ and to 0 for $\alpha = 1/10$, in agreement with theory.

against k (ϕ_0^h the numerical solution on the screen Γ_0, i.e. the solution for a unit square screen, this computed with 10000 DOFs corresponding to more than 6 DOFs/wavelength at the highest wavenumber $k = 100$). Here $\| \cdot \|_{\widetilde{H}_k^{-1/2}(\Gamma_j)}$ is a wavenumber-dependent norm on $\widetilde{H}^{-1/2}(\Gamma_j)$ commonly used in high frequency analysis (see the discussion in [22, §2.1]), given by

$$\|\psi\|_{\widetilde{H}_k^{-1/2}(\Gamma_j)}^2 = \int_{\mathbb{R}^{n-1}} (k^2 + |\boldsymbol{\xi}|^2)^{-1/2} |\widehat{\psi}(\boldsymbol{\xi})|^2 \, \mathrm{d}\boldsymbol{\xi}, \quad \psi \in \widetilde{H}^{-1/2}(\Gamma_j).$$

Clearly $\| \cdot \|_{\widetilde{H}_k^{-1/2}(\Gamma_j)}$ coincides with the standard norm for $k = 1$ and is equivalent to it for any fixed k, precisely [22, Eqn. (28)]

$$\min\left(1, k^{-1/2}\right) \|\psi\|_{\widetilde{H}^{-1/2}(\Gamma_j)} \leq \|\psi\|_{\widetilde{H}_k^{-1/2}(\Gamma_j)} \leq \max\left(1, k^{-1/2}\right) \|\psi\|_{\widetilde{H}^{-1/2}(\Gamma_j)}^2,$$

for $\psi \in \widetilde{H}^{-1/2}(\Gamma_j)$.

Plotting these wavenumber-dependent norms enables comparison with the theoretical bounds in [22] that are expressed in terms of these norms. It follows from
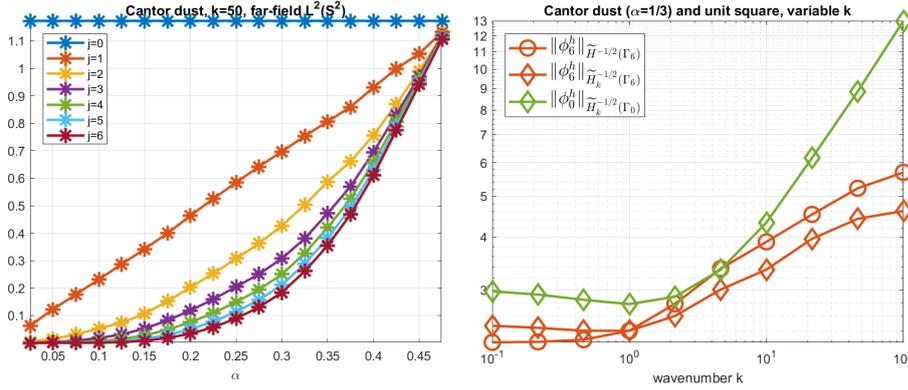
Fig. 12 Left: the $L^2(\mathbb{S}^2)$ norms of the far-field pattern for the Cantor dust, plotted against the parameter α, for standard prefractals of level $j = 0, 1, \ldots, 6$, computed with $N_j = 4096$ DOFs for each j. Proposition 6.2 implies that the limit for $j \to \infty$ is 0 for $\alpha \le 1/4$. Right: solution norms for $\alpha = 1/3$ and $j = 6$ (in red) and $j = 0$ (unit square, in green) as a function of the wavenumber k.

the coercivity and inhomogeneous term estimates in [22, Thms. 1.7, Lemma 6.1(i), (27)] that, for every value of j, $\|\phi_j\|_{\widetilde{H}_k^{-1/2}(\Gamma_j)}$ (ϕ_j the exact solution for the screen Γ_j) grows with increasing k at a rate no faster than $k^{1/2}$. In the results in the right panel $\|\phi_0^h\|_{\widetilde{H}_k^{-1/2}(\Gamma_0)}$, the solution for a unit square, grows for larger k at a rate $k^{0.48}$, while $\|\phi_6^h\|_{\widetilde{H}_k^{-1/2}(\Gamma_6)}$, the solution approximating the fractal limit, grows at a much more modest rate $k^{0.15}$. This suggests that the upper bounds in [22], which depend only on k and on the diameter of the screen, are sharp for large k in terms of their dependence on screen geometry for a regular screen, but are not sharp for screens with fractal dimension $< n - 1$.

7.5 Sierpinski triangle

We approximate the Sierpinski triangle with the standard prefractals Γ_j described in §6.3 (to be precise we mesh Γ_j°, the interior of Γ_j). We set $k = 40$, so that $\lambda \approx 0.157$ and the diameter of Γ is approximately 6.4 wavelengths, and consider a downward-pointing incoming wave with $\mathbf{d} = (0, 0, -1)$.

Figure 13 shows the near field and the magnitude of the (collocation) BEM solution ϕ_j^h for prefractal level $j = 8$ and $N_8 = 6561$ DOFs (one per component of Γ_j°). We note that $|\phi_j^h|$ achieves its maxima at the midpoints of the sides of the triangular holes of side length $1/8$, this size comparable with the wavelength λ.

Figure 14 (left panel) shows the solution norms for prefractal levels 0 to 8. In these computations we vary from our prescription in the results above of one DOF per component of the prefractal, using a larger number of elements at the lower prefractal levels to ensure that quadrature errors in the evaluation of the coefficients in the linear system are not significant with the 7-point quadrature rule that we use on triangular elements (see §7.1). Precisely, for prefractals Γ_0 to Γ_5 we use a mesh of equilateral triangles of side $h_j = 2^{-5}$. For Γ_5 to Γ_8 we use equilateral triangles of size $h_j = 2^{-j}$, i.e. with one DOF per component of
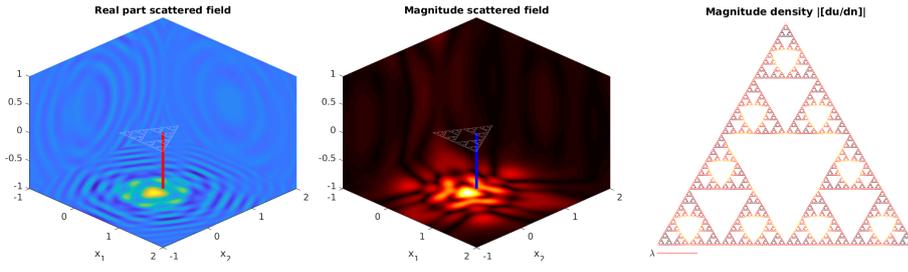
Fig. 13 Left and centre: the real part and magnitude of the field scattered by the level 8 prefractal approximation of the Sierpinski triangle, for the problem in §7.5, computed with $N_8 = 3^8 = 6561$ DOFs. Right: the magnitude $|\phi_j^h|$ of the piecewise constant BEM solution. Note that the peaks in $|\phi_j^h|$ (shown in yellow) are located close to the midpoints of the sides of the 9 triangular holes of size comparable to the wavelength (red segment).
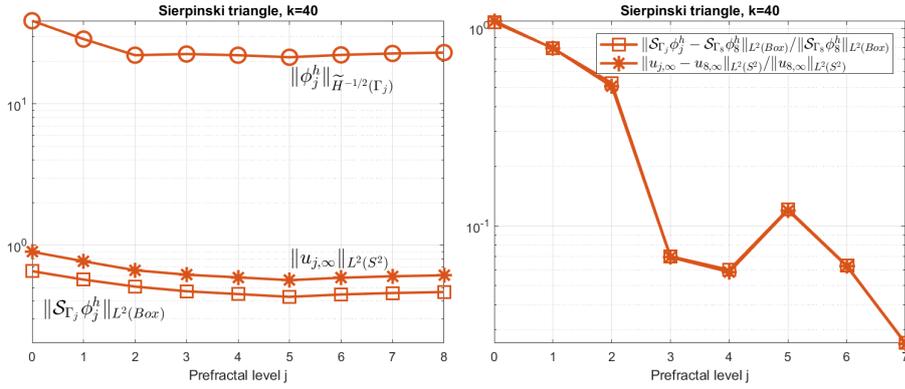
Fig. 14 Analogue of Figures 7 and 11 for the Sierpinski triangle, for the problem of §7.5, showing results for standard (non-thickened) prefractals only.

Γ_j°. The numbers of DOFs for $j = 0, \ldots, 8$ are $N_0 = 1024, N_1 = 768, N_2 = 576, N_3 = 432, N_4 = 324, N_5 = 243, N_6 = 729, N_7 = 2187, N_8 = 6561$. As in previous examples, we observe in the left panel rapid convergence of the norms to positive constant values. In the right panel we plot relative errors compared to the result for the finest prefractal Γ_8. As in the right panel of Figure 11 we see convergence which is exponential in j for $j \geq 5$. But the convergence is not monotonic in j for $j \leq 5$ where we fix h_j as we increase j.

7.6 Classical snowflakes

We now turn to examples in which the limiting screen Γ is a bounded open set with fractal boundary. In these cases, as $j \to \infty$ the area of the prefractals must tend to the (non-zero) area of the limiting screen. Thus, in our simulations based on uniform meshes, the cost increase associated with the increasingly fine mesh required to represent the prefractal boundary exactly as $j \to \infty$ will not be compensated by a decrease in the area to be meshed, as was the case for the Cantor sets/dusts and the Sierpinski triangle. This in turn means that our simulations based on uniform
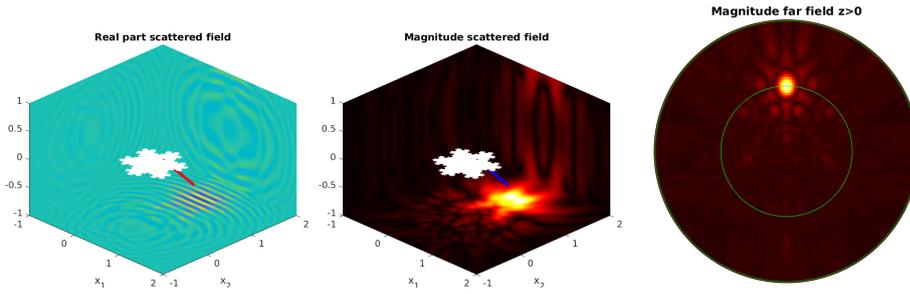
Fig. 15 The real part, magnitude and far-field pattern of the field scattered by the level 4 inner prefractal approximation Γ_4^- of the Koch snowflake, for the problem in §7.6, computed using a uniform BEM mesh with $N_4^- = 10344$ DOFs.

meshes and direct solvers will be more expensive than the numerical experiments reported above, limiting the prefractal level that can be attained. More efficient BEM approaches could be developed for these problems using appropriate non-uniform meshes such as those in [5, 19, 51], and/or fast iterative matrix-free linear solvers. But for brevity we leave such considerations to future work.

We consider first the standard Koch snowflake Γ with $\beta = \pi/6$ and $\xi = 1/3$, in the notation of §6.4. We approximate Γ with both the inner (open) and the outer (compact) prefractals Γ_j^- and Γ_j^+ defined in §6.4, on which we build uniform meshes conforming to the prefractal geometries (strictly, our mesh is on $(\Gamma_j^+)^\circ$ in the outer prefractal case). Figure 15 shows the scattered field for an incident plane wave with $k = 61$ (wavelength $\lambda \approx 0.103$) and $\mathbf{d} = (0, \frac{1}{\sqrt{2}}, -\frac{1}{\sqrt{2}})$, at inner prefractal level 4, computed with $N_4^- = 10344$ DOFs.

By Proposition 6.4, which relies on the fact that Γ is thick, so that $\widetilde{H}^{-1/2}(\Gamma) = H_{\overline{\Gamma}}^{-1/2}$, Galerkin BEM solutions for the inner and outer prefractals should both converge to the unique limiting solution on Γ, provided that $h_j \to 0$ as $j \to \infty$. We investigate this numerically (for the collocation BEM) in Figure 16 (though our simulations use a fixed h_j on each Γ_j^- and a fixed mesh size also on each Γ_j^+, as is described in more detail below). This figure shows that the alternating inner/outer sequence of prefractal approximations $\Gamma_0^-, \Gamma_0^+, \Gamma_1^-, \Gamma_1^+, \Gamma_2^-, \Gamma_2^+, \Gamma_3^-, \Gamma_3^+, \Gamma_4^-$ has the property that the $H^{-1/2}(\mathbb{R}^2)$ norm of the difference between the BEM solutions on consecutive prefractals in the sequence tends to zero monotonically (and approximately exponentially) as one moves along the sequence. The figure also suggests that plane waves hitting the screen perpendicularly lead to the lowest relative difference between solutions on inner and outer prefractals, that grazing incident waves lead to the largest difference, and that the relative errors are rather insensitive to the wavenumber for the values of k investigated.

For completeness we give a brief explanation of how the results in Figure 16 were computed. The inner prefractals Γ_j^- of levels $0 \le j \le 4$ are the union of 1, 12, 120, 1128 and 10344 equilateral triangles of side 3^{-j}, respectively. We mesh them all with equilateral triangles of the same side length $3^{-4} \approx 0.0123$, so that the total numbers of DOFs on the respective meshes M_j^- are $N_0^- = 6561 = 3^8$, $N_1^- = 8748 = 3^6 \cdot 12$, $N_2^- = 9720 = 3^4 \cdot 120$, $N_3^- = 10152 = 3^2 \cdot 1128$, and $N_4^- = 10344$. The outer prefractals Γ_j^+ of levels $0 \le j \le 3$ are the union of 6,

$$\|\phi_{j_{in}}^{h,-} - \phi_{j_{out}}^{h,+}\|_{H^{-1/2}(R^2)}/\|\phi_{j_{out}}^{h,+}\|_{H^{-1/2}(R^2)}$$
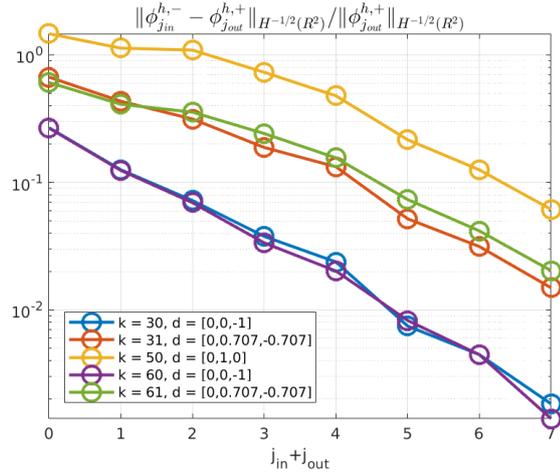
Fig. 16 The relative difference, measured in the $H^{-1/2}$ norm, between the BEM solutions on $\Gamma_{j_{in}}^-$ and on $\Gamma_{j_{out}}^+$, for $j_{in} + j_{out} = 0, 1, \ldots, 7$, with $j_{out} \in \{j_{in} - 1, j_{in}\}$, for the problem described in §7.6 (green curve). We show results also for four other similar problems with different values of k and either vertically, horizontally or obliquely incident plane waves.
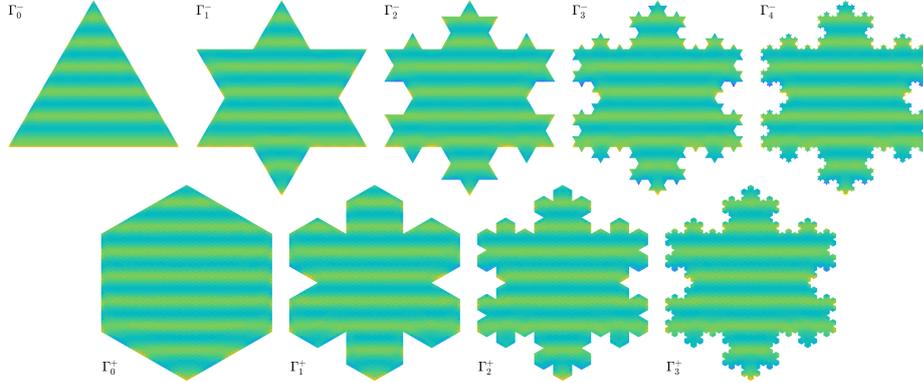
Fig. 17 The real part of the BEM solutions $\phi_j^{h,\pm}$ on the inner and outer prefractals $\Gamma_0^-, \ldots, \Gamma_4^-$ and $\Gamma_0^+, \ldots, \Gamma_3^+$ of the standard Koch snowflake, for the problem in §7.6. All plots are in the same colour scale.

48, 408 and 3576 equilateral triangles of side $3^{-j-\frac{1}{2}}$, respectively. We mesh them all with equilateral triangles of the same side length $3^{-\frac{7}{2}} \approx 0.0214$, so that the total numbers of DOFs on the respective meshes M_j^+ are $N_0^+ = 4374 = 3^6 \cdot 6$, $N_1^+ = 3888 = 3^4 \cdot 48$, $N_2^+ = 3672 = 3^2 \cdot 408$ and $N_3^+ = 3576$. Figure 17 shows the real part of the BEM solution $\phi_j^{h,\pm}$ for these prefractals and meshes.

To compute an approximation to the $H^{-1/2}(\mathbb{R}^2)$ norm of the difference $\phi_j^{h,-} - \phi_j^{h,+}$, as plotted in Figure 16, we first represent both piecewise-constant fields on the same mesh. We note that the equilateral triangles of M_j^+ are rotated by an angle of $\pi/2$ with respect to those of M_j^- and are larger by a (linear) factor $\sqrt{3}$.
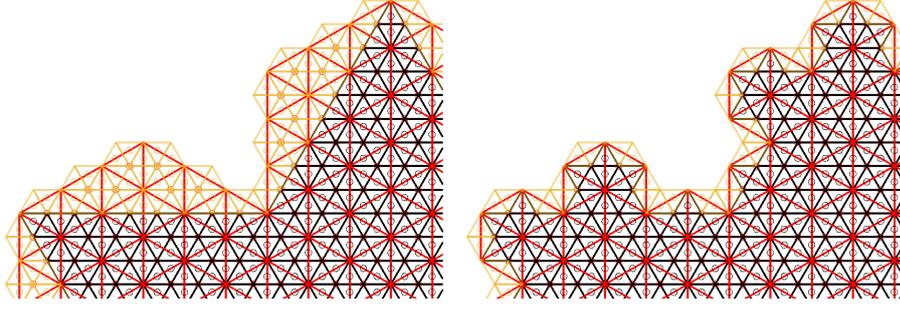
Fig. 18 Left: a portion of the meshes used to compute the norm of the difference of the BEM solutions ϕ_2^{h-} and ϕ_2^{h+} on the inner and the outer prefractals Γ_2^- and Γ_2^+. The black triangles are the elements of M_2^- and the red triangles are the elements of M_2^+. The circles denote the centres of the triangles of the same colour. The extended uniform mesh M_2^* is composed of the black and the yellow triangles, which cover the whole of Γ_2^+. Right: the analogous construction for the comparison between the solutions ϕ_4^{h-} and ϕ_3^{h+} on the prefractals Γ_4^- and Γ_3^+.

We define M_j^* to be the smallest uniform mesh that extends M_j^- and covers Γ_j^+; see Figure 18 for an illustration. We define two piecewise constant functions $\psi_j^\pm$ on this mesh. The first, ψ_j^-, is simply the zero-extension of ϕ_j^{h-}. The second, ψ_j^+, is defined from ϕ_j^{h+} as follows: noting that the centre of each element of M_j^* lies on an edge of M_j^+, we define the value of ψ_j^+ on $T_{j,l}^* \in M_j^*$ to be the average of the values of (the zero-extension of) ϕ_j^{h+} on the two triangles of (the uniform extension of) M_j^+ intersecting $T_{j,l}^*$. The norm $\|\psi_j^- - \psi_j^+\|_{H^{-1/2}(\mathbb{R}^2)}$ approximates $\|\phi_j^{h-} - \phi_j^{h+}\|_{H^{-1/2}(\mathbb{R}^2)}$ and can be computed using the reaction–diffusion single-layer operator as in the previous examples. To compute the norm of $\phi_{j+1}^{h-} - \phi_j^{h+}$ we proceed similarly.

7.7 Square snowflake

Finally, we consider the square snowflake Γ and the associated sequence of non-nested prefractals Γ_j described in §6.5. We choose $k = 40$ and $\mathbf{d} = (0, 0, -1)$. Plots of the resulting near- and far-field solutions for prefractal level $j = 3$ are shown in Figure 19. Proposition 6.5 implies that we have (Galerkin) BEM convergence provided $h_j \to 0$ as $j \to \infty$. But numerical validation of this convergence is hampered by the fact that the minimal number of DOFs required to discretise the jth-level prefractal with a uniform mesh of squares is 16^j. In order to simulate higher-level prefractals more sophisticated BEM implementations are needed, e.g. using fast matrix–vector multiplications, and non-uniform or non-convex meshes. This will be considered in future work.

8 Conclusion and open problems

In this paper we have written down in §3 well-posed BVP and BIE formulations for scattering by an acoustic screen Γ that is either fractal or has fractal boundary,
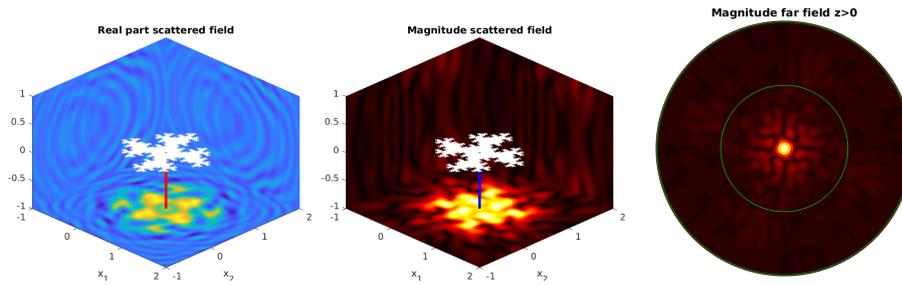
Fig. 19 Left and centre: the real part and magnitude of the field scattered by the level 3 prefractal approximation of the square snowflake, for the problem in §7.7, computed with $N_3 = 16^3 = 4096$ DOFs, i.e. ≈ 10 DOFs per wavelength. Right: the far-field pattern for the same problem.

refining, simplifying, and extending (in particular through application of recent results from [15]) the earlier results of [24]. Generalising the treatment in [24], we have studied in §4 (using Mosco convergence for the first time in this context) the convergence of BIE solutions on a sequence of prefractals Γ_j to the solution on a limiting set Γ; in particular we have proved in Theorem 4.1 and Proposition 4.3 new convergence results in cases where the sequence of prefractals Γ_j is not monotonically convergent to Γ, and have applied these results in §4.1 to sequences of prefractals generated by general iterated function systems.

But the crucial novelty of the paper has been the analysis and implementation of the BEM in §§5–7. In §4.1 we have obtained, to our knowledge, the first rigorous convergence analysis of a numerical method for scattering by a fractal object and the first proofs of convergence of BEM, applied on a sequence of prefractal sets Γ_j, to the solution of the BIE on the limiting set Γ, both in cases when Γ is fractal (in particular the fixed point of an IFS of contracting similarities satisfying the standard open set condition, for example the Cantor set or dust, the Sierpinski triangle) and in cases where Γ is an open set with fractal boundary (for example the Koch or square snowflake). We have studied these specific cases as examples of applying these new convergence results in §6, and in numerical experiments in §7.

These results are, we consider, important first steps in understanding BIEs and their solutions on sets that are fractal or have fractal boundary, and the convergence to these solutions of BEM approximations on sequences of more regular prefractals. More generally, these results and methods are applicable to the convergence analysis of Galerkin methods for BIEs (and, we anticipate, other integral equations and PDEs) posed on *any* rough domain that cannot be discretised exactly but first needs to be approximated by a sequence of more regular sets.

For the specific screen scattering problems that have been the focus of this paper, and for large classes of related problems, there remain many intriguing and important open questions. These include:

1. What is the regularity of the BIE solution on the limiting screen Γ, and how does this depend on the fractal dimension of Γ or its boundary? In the case when Γ is fractal the density results summarised in Lemma 3.13 are one step towards addressing this question.

2. At what rate do BIE solutions on a prefractal sequence Γ_j converge to the limiting BIE solution on Γ?
3. If the BIE is additionally discretised by BEM, how does the convergence rate depend jointly on the prefractal level j and the discretisation? (The numerical simulations in §7 provide some experimental data.)
4. Extending this question, what is the optimal balance (to achieve an accurate approximation of the solution on Γ with least work) between increasing the prefractal level and mesh refinement? For example, for the family of pre-convex meshes (42), what is the optimal choice of the parameter $i(j)$?

We hope to address some of these questions in future work, together with exploring more efficient BEM implementations (e.g. using locally-refined meshes, fast iterative solvers for structured meshes), and the extension of the methods developed here to more general problems (e.g. curvilinear screens, different boundary conditions, elastic and electromagnetic waves, other PDEs).

9 Acknowledgements

A Finite element approximation by piecewise constants

Let $m \in \mathbb{N}$ and $\Omega \subset \mathbb{R}^m$ be a non-empty bounded open set. Let us say that M is a *pre-convex mesh* on Ω if, for some $N \in \mathbb{N}$, $M = \{T_1, T_2, \ldots, T_N\}$ is a collection of open subsets $T_j \subset \Omega$ such that: (i) the convex hulls $\mathrm{Conv}(T_j)$ are pairwise disjoint; (ii) each ∂T_j has zero m-dimensional Lebesgue measure; and (iii) $\Omega = \left(\overline{\bigcup_{j=1}^{N} T_j} \right)^\circ$. We note that (ii) holds (and this will be the case in the applications that we make) if each T_j is the union of a finite number of pairwise disjoint Lipschitz open sets, in particular if each T_j is convex, in which case we term M a *convex mesh*.

In the case that Ω is a curvilinear Lipschitz polygon and each T_j is a curvilinear triangle or quadrilateral, the following lemma is a standard BEM error estimate (e.g. [69, Thm. 10.4, (10.10)]), except that in the standard versions the explicit constant π^{s-t} in (44) is replaced by an unknown constant that depends (in an unspecified way) on the domain and the shape regularity of the elements. The version we prove here, which applies to any bounded open set Ω and any pre-convex mesh M, and provides explicit constants independent of the domain and element shape, should be of some independent interest and is essential for our application to BEM on sequences of prefractals converging to a fractal limit.

Lemma A.1. *Let $m \in \mathbb{N}$ and $N \in \mathbb{N}$, and let $\Omega \subset \mathbb{R}^m$ be a non-empty bounded open set and $M = \{T_1, T_2, \ldots, T_N\}$ be a pre-convex mesh on Ω. Let $V \subset L^2(\Omega)$ denote the set of piecewise constant functions on M, so that $u \in V$ if $u \in L^2(\Omega)$ and $u|_{T_j}$ is constant, for $j = 1, \ldots, N$. Let $\Pi : L^2(\Omega) \to V$ be orthogonal projection, so that*

$$(\Pi u)|_{T_j} = \frac{1}{|T_j|} \int_{T_j} u(\mathbf{x}) \, \mathrm{d}\mathbf{x}, \quad j = 1, \ldots, N.$$

Let $h := \max_{T \in M} \operatorname{diam}(T)$. Then, for $-1 \le s \le 0$ and $0 \le t \le 1$, if $u \in H^t(\Omega)$, then

$$\|u - \Pi u\|_{\widetilde{H}^s(\Omega)} \le (h/\pi)^{t-s} \|u\|_{H^t(\Omega)}, \tag{44}$$

where on the left hand side we extend $u - \Pi u$ from Ω to $\mathbb{R}^m$ by zero to become an element of $\widetilde{H}^0(\Omega) \subset \widetilde{H}^s(\Omega)$.

Proof. Clearly (44) holds for $s = t = 0$ as $H^0(\Omega) = L^2(\Omega)$, with identical norms, and Π is an orthogonal projection operator on $L^2(\Omega)$. Now suppose that $s = 0$ and $t = 1$. In this case, recalling that $\widetilde{H}^0(\Omega) = \overline{C_0^\infty(\Omega)}^{L^2(\mathbb{R}^m)} = L^2(\Omega)$ with equal norms, and that $\|u\|_{H^1(\Omega)} = \min_{U \in H^1(\mathbb{R}^m), \, u = U|_\Omega} \|U\|_{H^1(\mathbb{R}^m)}$, the required bound (44) is implied by

$$\|u - \Pi u\|_{L^2(\Omega)} \le \frac{h}{\pi} \|\nabla U\|_{L^2(\mathbb{R}^m)}, \tag{45}$$

where $U \in H^1(\mathbb{R}^m)$ is such that $u = U|_\Omega$ and $\|u\|_{H^1(\Omega)} = \|U\|_{H^1(\mathbb{R}^m)}$. To see that this bound holds, let T_j^H denote the convex hull of T_j, for $j = 1, \ldots, N$, which has the same diameter as T_j, and let $\Omega^H := \left(\bigcup_{j=1}^N \overline{T_j^H} \right)^\circ$, so that $M^H := \{T_1^H, \ldots, T_N^H\}$ is a convex mesh on Ω^H. Let $V^H \subset L^2(\Omega^H)$ denote the space of piecewise constant functions on M^H, $\Pi^H : L^2(\Omega^H) \to V^H$ be orthogonal projection, and $u^H := U|_{\Omega^H}$. Then $(\Pi^H u^H)|_\Omega \in V$ so that

$$\|u - \Pi u\|_{L^2(\Omega)}^2 \le \|u - (\Pi^H u^H)|_\Omega\|_{L^2(\Omega)}^2$$

$$\le \|u^H - \Pi^H u^H\|_{L^2(\Omega^H)}^2 = \sum_{j=1}^N \|(u^H - \Pi^H u^H)|_{T_j^H}\|_{L^2(T_j^H)}^2.$$

But

$$\|(u^H - \Pi^H u^H)|_{T_j^H}\|_{L^2(T_j^H)} \le C \|(\nabla U)|_{T_j^H}\|_{L^2(T_j^H)}$$

for some $C > 0$, by the standard Poincaré inequality. Indeed, since T_j^H is convex, this bound holds with $C = h_j/\pi$, where $h_j = \operatorname{diam}(T_j) = \operatorname{diam}(T_j^H)$, which is known [8,60] to be the best constant in this inequality for convex domains. The inequality (45) follows since the T_H^j are pairwise disjoint.

Thus (44) is proved for $s = 0$ and $t = 0, 1$, and by interpolation it extends to $s = 0$ and $0 < t < 1$. Precisely, let $\| \cdot \|_t$ denote the norm on the K-method interpolation space $K_{t,2}((L^2(\Omega), H^1(\Omega)))$, with the normalisation defined in [25, (7,8)]. Then

$$\|u - \Pi u\|_{L^2(\Omega)} \le (h/\pi)^t \|u\|_t \le (h/\pi)^t \|u\|_{H^t(\Omega)}, \quad 0 < t < 1, \tag{46}$$

where the first inequality follows by interpolation since $K_{t,2}((L^2(\Omega), L^2(\Omega))) = L^2(\Omega)$ with equality of norms given the normalisation [25, (7,8)] (see [25, Lem. 2.1(iii), Thm. 2.2(i)]); the second inequality holds since, again given this normalisation, the embedding of $H^t(\Omega)$ into $K_{t,2}((L^2(\Omega), H^1(\Omega)))$ has norm ≤ 1 [25, Lem. 4.2].

Finally, suppose that $-1 \le s < 0$ and $0 \le t \le 1$. Then, as $H^{-s}(\Omega)$ is a unitary realisation of the dual space of $\widetilde{H}^s(\Omega)$ via an extension of the $L^2(\Omega)$ inner product, if $u \in H^t(\Omega)$ then

$$\|u - \Pi u\|_{\widetilde{H}^s(\Omega)} = \sup_{0 \ne v \in H^{-s}(\Omega)} \frac{|(u - \Pi u, v)_{L^2(\Omega)}|}{\|v\|_{H^{-s}(\Omega)}}$$

$$= \sup_{0 \ne v \in H^{-s}(\Omega)} \frac{|(u - \Pi u, v - \Pi v)_{L^2(\Omega)}|}{\|v\|_{H^{-s}(\Omega)}} \le (h/\pi)^{t-s} \|u\|_{H^t(\Omega)},$$

where the final bound follows from the Cauchy–Schwarz inequality and two applications of (46). $\square$

B Mollification and Sobolev regularity

Given $m \in \mathbb{N}$, choose $\psi \in C_0^\infty(\mathbb{R}^m)$ with $\psi(\mathbf{x}) = 0$ for $|\mathbf{x}| > 1$ and $\int_{\mathbb{R}^m} \psi(\mathbf{x})\mathrm{d}\mathbf{x} = 1$, and for $\epsilon > 0$ let

$$\psi_\epsilon(\mathbf{x}) := \epsilon^m \psi(\mathbf{x}/\epsilon), \quad \mathbf{x} \in \mathbb{R}^m.$$

Given $s \in \mathbb{R}$, for $\phi \in H^s(\mathbb{R}^m)$ and $\epsilon > 0$ we define ϕ_ϵ, the ϵ-mollification of ϕ, by $\phi_\epsilon := \psi_\epsilon * \phi$, where

$$\psi_\epsilon * \phi(\mathbf{x}) := \int_{\mathbb{R}^m} \psi_\epsilon(\mathbf{x} - \mathbf{y})\phi(\mathbf{y})\,\mathrm{d}\mathbf{y}, \quad \mathbf{x} \in \mathbb{R}^m,$$

in the case that $\phi \in L^2(\Gamma)$, and, in the case that $s < 0$, the definition of $\psi_\epsilon * \phi$ is extended to all $\phi \in H^s(\mathbb{R}^m)$ by continuity and density. It is standard that $\phi_\epsilon \to \phi$ in $H^s(\mathbb{R}^m)$ as $\epsilon \to 0$ (e.g. [52, Exercise 3.17]). Moreover, with the Fourier transform normalised as in §2.4, we have that

$$\widehat{\psi_\epsilon}(\boldsymbol{\xi}) = \widehat{\psi}(\epsilon\boldsymbol{\xi}) \qquad \text{and} \qquad \widehat{\phi_\epsilon}(\boldsymbol{\xi}) = c_m \widehat{\psi_\epsilon}(\boldsymbol{\xi})\widehat{\phi}(\boldsymbol{\xi}), \quad \text{for } \boldsymbol{\xi} \in \mathbb{R}^m,$$

where $c_m := (2\pi)^{m/2}$. Hence it holds for $t \geq s$ that

$$\|\phi_\epsilon\|_{H^t(\mathbb{R}^m)}^2 = c_m^2 \int_{\mathbb{R}^m} |\widehat{\psi}(\epsilon\boldsymbol{\xi})|^2\,|\widehat{\phi}(\boldsymbol{\xi})|^2 (1 + \boldsymbol{\xi}^2)^{t/2}\,\mathrm{d}\boldsymbol{\xi} \leq c_m^2 C_\epsilon^2\,\|\phi\|_{H^s(\mathbb{R}^m)}^2,$$

where

$$C_\epsilon := \sup_{\boldsymbol{\xi} \in \mathbb{R}^m} \left| \widehat{\psi}(\epsilon\boldsymbol{\xi})(1 + \boldsymbol{\xi}^2)^{(t-s)/2} \right| = \sup_{\boldsymbol{\xi} \in \mathbb{R}^m} \left| \widehat{\psi}(\boldsymbol{\xi})(1 + (\boldsymbol{\xi}/\epsilon)^2)^{(t-s)/2} \right|.$$

Since $\psi \in C_0^\infty(\mathbb{R}^m)$, it holds for $0 < \epsilon \leq 1$ that

$$C_\epsilon \leq c'_{t-s} \sup_{\boldsymbol{\xi} \in \mathbb{R}^m} \left(\frac{1 + \boldsymbol{\xi}^2/\epsilon^2}{1 + \boldsymbol{\xi}^2} \right)^{(t-s)/2} \leq c'_{t-s}\,\epsilon^{s-t}, \text{ where } c'_p := \max_{\boldsymbol{\xi} \in \mathbb{R}^m} |\widehat{\psi}(\boldsymbol{\xi})|(1 + \boldsymbol{\xi}^2)^{p/2},$$

for $p \geq 0$. Thus, for $t \geq s$, $\epsilon > 0$, and $\phi \in H^s(\mathbb{R}^m)$, it holds that

$$\|\phi_\epsilon\|_{H^t(\mathbb{R}^m)} \leq c_m c'_{t-s}\,\epsilon^{s-t}\,\|\phi\|_{H^s(\mathbb{R}^m)}. \tag{47}$$

References

1. Y. ACHDOU, C. SABOT, AND N. TCHOU, *Transparent boundary conditions for the Helmholtz equation in some ramified domains with a fractal boundary*, J. Comput. Phys., 220 (2007), pp. 712–739.
2. E. A. ALGEHYNE AND A. J. MULHOLLAND, *A finite element approach to modelling fractal ultrasonic transducers*, IMA J. Appl. Math., 80 (2015), pp. 1684–1702.
3. E. A. ALGEHYNE AND A. J. MULHOLLAND, *Analysis of a fractal ultrasonic transducer with a range of piezoelectric length scales*, IMA J. Appl. Math., 84 (2019), pp. 605–631.
4. K. ARFI AND A. ROZANOVA-PIERRAT, *Dirichlet-to-Neumann or Poincaré-Steklov operator on fractals described by d-sets*, Discret. Contin. Dyn. S., 12 (2019), pp. 1–26.
5. P. BAGNERINI, A. BUFFA, AND E. VACCA, *Mesh generation and numerical analysis of a Galerkin method for highly conductive prefractal layers*, Appl. Numer. Math., 65 (2013), pp. 63–78.
6. L. BANJAI AND L. BOULTON, *The Poincaré constant of the Koch snowflake*, arXiv preprint arXiv:1708.08401, (2017).
7. A. J. BARAN, *A review of the light scattering properties of cirrus*, J. Quant. Spectrosc. Ra., 110 (2009), pp. 1239–1260.
8. M. BEBENDORF, *A note on the Poincaré inequality for convex domains*, Z. Anal. Anwend., 22 (2003), pp. 751–756.
9. F. BEN HASSEN, Y. BOUKARI, AND H. HADDAR, *Application of the linear sampling method to identify cracks with impedance boundary conditions*, Inverse Probl. Sci. En., 21 (2013), pp. 210–234.
10. M. V. BERRY, *Diffractals*, J. Phys. A: Math. Gen., 12 (1979), p. 781.
11. A. BESPALOV, N. HEUER, AND R. HIPTMAIR, *Convergence of the natural hp-BEM for the electric field integral equation on polyhedral surfaces*, SIAM J. Numer. Anal., 48 (2010), pp. 1518–1529.

12. C. J. Bouwkamp, *Diffraction theory*, Rep. Prog. Phys., 17 (1954), pp. 35–100.
13. D. Bucur and N. Varchon, *Boundary variation for a Neumann problem*, Ann. Scuola Norm. Sup. Pisa Cl. Sci. (4), 29 (2000), pp. 807–821.
14. A. Buffa and S. H. Christiansen, *The electric field integral equation on Lipschitz screens: definitions and numerical approximation*, Numer. Math., 94 (2003), pp. 229–267.
15. A. Caetano, D. P. Hewett, and A. Moiola, *Density results for Sobolev, Besov and Triebel-Lizorkin spaces on rough sets*, arXiv:1904.05420, (2018).
16. R. Capitanelli and M. Vivaldi, *FEM for quasilinear obstacle problems in bad domains*, ESAIM: Math. Model. Num., 51 (2017), pp. 2465–2485.
17. R. Capitanelli and M. A. Vivaldi, *Weighted estimates on fractal domains*, Mathematika, 61 (2015), pp. 370–384.
18. M. Cefalo, M. Lancia, and H. Liang, *Heat-flow problems across fractal mixtures: regularity results of the solutions and numerical approximation*, Differ. Integral Equ., 26 (2013), pp. 1027–1054.
19. M. Cefalo and M. R. Lancia, *An optimal mesh generation algorithm for domains with Koch type boundaries*, Math. Comput. Simulat., 106 (2014), pp. 133–162.
20. R. Ceolato, M. J. Berg, and N. Riviere, *Spectral and angular light-scattering from silica fractal aggregates*, J. Quant. Spectrosc. Ra., 131 (2013), pp. 160–165.
21. S. Chandler-Wilde and M. Lindner, *Coburn's lemma and the finite section method for random Jacobi operators*, J. Funct. Anal., 270 (2016), pp. 802–841.
22. S. N. Chandler-Wilde and D. P. Hewett, *Wavenumber-explicit continuity and coercivity estimates in acoustic scattering by planar screens*, Integr. Equat. Oper. Th., 82 (2015), pp. 423–449.
23. S. N. Chandler-Wilde and D. P. Hewett, *BVP and BIE formulations for scattering by fractal screens*, in Proc. 13th Int. Conf. on Mathematical and Numerical Aspects of Wave Propagation, Minneapolis, USA, 2017, pp. 85–90.
24. S. N. Chandler-Wilde and D. P. Hewett, *Well-posed PDE and integral equation formulations for scattering by fractal screens*, SIAM J. Math. Anal., 50 (2018), pp. 677–717.
25. S. N. Chandler-Wilde, D. P. Hewett, and A. Moiola, *Interpolation of Hilbert and Sobolev spaces: quantitative estimates and counterexamples*, Mathematika, 61 (2015), pp. 414–443.
26. S. N. Chandler-Wilde, D. P. Hewett, and A. Moiola, *Sobolev spaces on non-Lipschitz subsets of $\mathbb{R}^n$ with application to boundary integral equations on fractal screens*, Integr. Equat. Operat. Th., 87 (2017), pp. 179–224.
27. J. M. Christian, G. S. McDonald, A. Kotsampaseris, and J. Huang, *Fresnel diffraction patterns from fractal apertures: boundary conditions and circulation, pentaflakes and islands*, in Proceedings of EOSAM 2016, Berlin, Germany, European Optical Society, 2016.
28. X. Claeys and R. Hiptmair, *Integral equations on multi-screens*, Integr. Equat. Oper. Th., 77 (2013), pp. 167–197.
29. D. Colton and R. Kress, *Inverse Acoustic and Electromagnetic Scattering Theory*, Springer, 2nd ed., 1998.
30. J. B. Conway, *A Course in Functional Analysis*, Springer, 2nd ed., 1990.
31. M. Durand, *Layer potentials and boundary value problems for the Helmholtz equation in the complement of a thin obstacle*, Math. Meth. Appl. Sci., 5 (1983), pp. 389–421.
32. E. Evans, *A finite element approach to H^1 extension using prefractals*, Adv. Math. Sci. Appl, 22 (2012), pp. 391–420.
33. K. Falconer, *Fractal Geometry: Mathematical Foundations and Applications*, Wiley, 3rd ed., 2014.
34. H. Fang, Z. Qiu, A. Mulholland, R. O'Leary, and A. Gachagan, *Broadband 1-3 piezoelectric composite transducer design using Sierpinski gasket fractal geometry*, IEEE T. Ultrason. Ferr., 65 (2018), pp. 2429–2439.
35. B. Ghosh, S. N. Sinha, and M. V. Kartikeyan, *Fractal Apertures in Waveguides, Conducting Screens and Cavities*, Springer, 2014.
36. D. S. Grebenkov and B.-T. Nguyen, *Geometrical structure of Laplacian eigenfunctions*, SIAM Review, 55 (2013), pp. 601–667.
37. P. Grisvard, *Elliptic Problems in Nonsmooth Domains*, Pitman, 1985.
38. T. Ha-Duong, *On the transient acoustic scattering by a flat object*, Japan J. Indust. Appl. Math., 7 (1990), pp. 489–513.
39. D. P. Hewett and J. Bannister, *Acoustic scattering by impedance screens with fractal boundary*, in Proc. 14th Int. Conf. on Mathematical and Numerical Aspects of Wave Propagation, Vienna, Austria, 2019, pp. 80–81.

40. D. P. Hewett, S. Langdon, and S. N. Chandler-Wilde, *A frequency-independent boundary element method for scattering by two-dimensional screens and apertures*, IMA J. Numer. Anal., 35 (2015), pp. 1698–1728.

41. D. P. Hewett and A. Moiola, *On the maximal Sobolev regularity of distributions supported by subsets of Euclidean space*, Anal. Appl., 15 (2017), pp. 731–770.

42. H. Holm, M. Maischak, and E. P. Stephan, *The hp-version of the boundary element method for Helmholtz screen problems*, Computing, 57 (1996), pp. 105–134.

43. P. Horváth, P. Šmíd, I. Vašková, and M. Hrabovskỳ, *Koch fractals in physical optics and their Fraunhofer diffraction patterns*, Optik, 121 (2010), pp. 206–213.

44. C. Hua and B. Sleeman, *High-frequency estimates for the Neumann scattering phase in non-smooth obstacle scattering*, Inverse Probl., 17 (2001), p. 1.

45. F. Ihlenburg, *Finite Element Analysis of Acoustic Scattering*, Springer, 1998.

46. A. D. Jaggard and D. L. Jaggard, *Cantor ring diffractals*, Opt. Commun., 158 (1998), pp. 141–148.

47. P. Joly and A. Semin, *Mathematical and numerical modeling of wave propagation in fractal trees*, C. R. Acad. Sci. I-Math., 349 (2011), pp. 1047–1051.

48. P. Jones, J. Ma, and V. Rokhlin, *A fast direct algorithm for the solution of the Laplace equation on regions with fractal boundaries*, J. Comput. Phys., 113 (1994), pp. 35–51.

49. T. Kato, *Perturbation Theory for Linear Operators*, Springer, corrected printing of 2nd ed., 1995.

50. R. Kress and K.-M. Lee, *Integral equation methods for scattering from an impedance crack*, J. Comput. Appl. Math., 161 (2003), pp. 161–177.

51. M. R. Lancia, M. Cefalo, and G. DellAcqua, *Numerical approximation of transmission problems across Koch-type highly conductive layers*, Appl. Math. Comput., 218 (2012), pp. 5453–5473.

52. W. McLean, *Strongly Elliptic Systems and Boundary Integral Equations*, CUP, 2000.

53. G. Menegatti and L. Rondi, *Stability for the acoustic scattering problem for sound-hard scatterers*, Inverse Probl. Imaging, 7 (2013), pp. 1307–1329.

54. U. Mosco, *Convergence of convex sets and of solutions of variational inequalities*, Advances in Mathematics, 3 (1969), pp. 510–585.

55. U. Mosco, *An introduction to the approximate solution of variational inequalities*, in Constructive Aspects of Functional Analysis, G. Geymonat, ed., C.I.M.E., Ed. Cremonese, Roma, 1971, pp. 497–682.

56. U. Mosco, *Analysis and numerics of some fractal boundary value problems*, in Analysis and Numerics of Partial Differential Equations, F. Brezzi, P. Colli Franzone, U. Gianazza, and G. Gilardi, eds., Springer, 2013, pp. 237–255.

57. A. J. Mulholland and A. J. Walker, *Piezoelectric ultrasonic transducers with fractal geometry*, Fractals, 19 (2011), pp. 469–479.

58. J. M. Neuberger, N. Sieben, and J. W. Swift, *Computing eigenfunctions on the Koch snowflake: A new grid and symmetry*, J. Comput. Appl. Math., 191 (2006), pp. 126–142.

59. P. Panagiotopoulos and O. Panagouli, *The BEM in plates with boundaries of fractal geometry*, Eng. Anal. Bound. Elem., 17 (1996), pp. 153–160.

60. L. E. Payne and H. F. Weinberger, *An optimal Poincaré inequality for convex domains*, Arch. Rational Mech. Anal., 5 (1960), pp. 286–292.

61. C. Puente-Baliarda, J. Romeu, R. Pous, and A. Cardama, *On the behavior of the Sierpinski multiband fractal antenna*, IEEE T. Antenn. Propag., 46 (1998), pp. 517–524.

62. A. Quarteroni, R. Sacco, and F. Saleri, *Numerical mathematics*, Springer, 2nd ed., 2007.

63. W. Rudin, *Functional Analysis*, McGraw-Hill, 2nd ed., 1991.

64. B. Sapoval, T. Gobron, and A. Margolina, *Vibrations of fractal drums*, Phys. Rev. Lett., 67 (1991), p. 2974.

65. B. Sleeman and C. Hua, *An analogue of Berry's conjecture for the phase in fractal obstacle scattering*, IMA J. Appl. Math., 49 (1992), pp. 193–202.

66. W. Śmigaj, T. Betcke, S. Arridge, J. Phillips, and M. Schweiger, *Solving boundary integral problems with BEM++*, ACM Trans. Math. Software, 41 (2015), pp. Art. 6, 40.

67. V. P. Smyshlyaev and E. A. Spence, *Coercivity of boundary integral equations in high frequency scattering*, in Proceedings of the 10th International Conference on the Mathematical and Numerical Aspects of Waves, Vancouver, Canada, July 2011.

68. T. H. M. Stein, C. D. Westbrook, and J. C. Nicol, *Fractal geometry of aggregate snowflakes revealed by triple-wavelength radar measurements*, Geophys. Res. Lett., 42 (2015), pp. 176–183.

69. O. Steinbach, *Numerical Approximation Methods for Elliptic Boundary Value Problems*, Springer, 2008.

70. E. P. Stephan, *Boundary integral equations for screen problems in* $\mathbb{R}^3$, Integr. Equat. Oper. Th., 10 (1987), pp. 236–257.

71. E. P. Stephan and W. L. Wendland, *An augmented Galerkin procedure for the boundary integral method applied to two-dimensional screen and crack problems*, Appl. Anal., 18 (1984), pp. 183–219.

72. H. Triebel, *Fractals and Spectra*, Birkhäuser, 1997.

73. H. Triebel, *Function spaces and wavelets on domains*, EMS, 2008.

74. J. Tyynelä, J. Leinonen, D. Moisseev, and T. Nousiainen, *Radar backscattering from snowflakes: Comparison of fractal, aggregate, and soft spheroid models*, J. Atmos. Ocean. Tech., 28 (2011), pp. 1365–1372.

75. R. Verma, M. K. Sharma, V. Banerjee, and P. Senthilkumaran, *Robustness of Cantor diffractals*, Opt. Express, 21 (2013), pp. 7951–7956.

76. W. L. Wendland and E. P. Stephan, *A hypersingular boundary integral method for two-dimensional screen and crack problems*, Arch. Rational Mech. Anal., 112 (1990), pp. 363–390.

77. D. H. Werner and S. Ganguly, *An overview of fractal antenna engineering research*, IEEE Antenn. Propag. M., 45 (2003), pp. 38–57.